AD_____

Award Number: DAMD17-02-1-0490

TITLE: Detection of Metastatic Potential in Breast Cancer by RhoC-GTPase and WISP3 Proteins

PRINCIPAL INVESTIGATOR: Celina G. Kleer, M.D.

CONTRACTING ORGANIZATION: The University of Michigan
Ann Arbor, Michigan 48109-1274

REPORT DATE: May 2004

TYPE OF REPORT: Annual

PREPARED FOR: U.S. Army Medical Research and Materiel Command
Fort Detrick, Maryland 21702-5012

REPORT DOCUMENTATION PAGE

Form Approved
OMB No. 074-0188

1. AGENCY USE ONLY (Leave blank)	2. REPORT DATE	3. REPORT TYPE AND DATES COVERED
	May 2004	Annual (17 Apr 2003 - 16 Apr 2004)

4. TITLE AND SUBTITLE
Detection of Metastatic Potential in Breast Cancer by RhoC-GTPase and WISP3 Proteins

5. FUNDING NUMBERS
DAMD17-02-1-0490

6. AUTHOR(S)
Celina G. Kleer, M.D.

7. PERFORMING ORGANIZATION NAME(S) AND ADDRESS(ES)
The University of Michigan
Ann Arbor, Michigan 48109-1274

E-Mail: kleer@umich.edu

8. PERFORMING ORGANIZATION REPORT NUMBER

9. SPONSORING / MONITORING AGENCY NAME(S) AND ADDRESS(ES)
U.S. Army Medical Research and Materiel Command
Fort Detrick, Maryland 21702-5012

10. SPONSORING / MONITORING AGENCY REPORT NUMBER

11. SUPPLEMENTARY NOTES
Original contains color plates: All DTIC reproductions will be in black and white.

12a. DISTRIBUTION / AVAILABILITY STATEMENT
Approved for Public Release; Distribution Unlimited

12b. DISTRIBUTION CODE

13. ABSTRACT (Maximum 200 Words)
Breast cancer is the most common type of life-threatening cancer, and the second most common cause of cancer related deaths of women in the United States. Even though the larger the primary tumor, the greater the likelihood of metastases, this is not always the case. There are many small breast cancers with a highly aggressive and metastatic behavior and discouraging outcome that remain under treated because there is no marker capable of identifying them. In this proposal we will study the utility of detecting RhoC GTPase and WISP3 proteins by immunohistochemistry as biological prognostic markers capable of identifying breast cancers with high propensity to metastasize, independently of tumor size. The impact of this study is that we will develop a clinically useful test to detect which invasive cancers will metastasize, and that will allow clinicians to institute early treatment before the development of metastases. This will impact on patient outcome. We will also study the predictive power of RhoC GTPase and WISP3 expression in the response of breast cancer to farnesyl transferase inhibitors, a new gene-targeted treatment modality for advanced cancers.

14. SUBJECT TERMS
WISP3, inflammatory breast cancer, RhoC-GTPase, prognostic factor

15. NUMBER OF PAGES
42

16. PRICE CODE

17. SECURITY CLASSIFICATION OF REPORT	18. SECURITY CLASSIFICATION OF THIS PAGE	19. SECURITY CLASSIFICATION OF ABSTRACT	20. LIMITATION OF ABSTRACT
Unclassified	Unclassified	Unclassified	Unlimited

Table of Contents

Celina G. Kleer, M.D.
Annual Report for Award Number: DAMD17-02-1-0490
Career Development Award
May 2004 (Reporting period 17 April 2003- 16 April 2004)

Introduction

This is a the second annual report for a project that aims at understanding the clinical utility of RhoC-GTPase and WISP3 proteins in breast cancer patients. These two genes were identified as key genetic determinants of inflammatory breast cancer (IBC). We believe that RhoC GTPase and WISP3 act in concert to determine a highly metastatic breast cancer phenotype, and that they may help identify which invasive breast carcinomas are aggressive from the outset and treat them more appropriately before the development of metastases. Specifically, we aim to determine whether detection of RhoC GTPase and WISP3 proteins in breast cancer tissue samples can identify aggressive tumors. A second goal of our award is to determine the effect of farnesyl transferase inhibitors (FTIs) in RhoC overexpressing xenografts. We have made significant progress in the last year, which is summarized below:

Body

The major thrusts of our year's work have been to better understand the functional significance of the WISP3 gene in Inflammatory Breast Cancer (IBC), to determine the prognostic utility of RhoC protein expression in a large group of breast cancer tissues, and to develop and optimize key reagents to test the clinical utility of WISP3 in breast cancer tissue samples. Below are brief descriptions of key accomplishments according to the approved statement of work (SOW):

Task 1. To determine whether the concordant alterations of RhoC-GTPase over-expression and WISP3 loss are prognostic indicators of a more aggressive phenotype in breast cancer. Months 1-24.

a. Identify and retrieve the breast cancer tissue blocks and slides (400 cases total). Months 1-6.
b. Histopathologic study of the cases and selection of adequate tumor areas to construct the tissue microarrays. Categorize the breast cancers according to stage. Months 6-9.
c. Construction of the tissue microarrays containing 400 breast cancers of all anatomic stages. Months 9-15.
d. Immunohistochemical analysis for RhoC-GTPase and WISP3 proteins, and other markers (ER, PR, HER2/neu, Ki-67, microvessel density and apoptosis). Months 16-19.
e. Interpretation and grading of the immunohistochemical studies and statistical analyses. Months 20-24

Task 1

a. Identify and retrieve the breast cancer tissue blocks and slides.
By performing a computerized search of the breast cancer database at the Department of Pathology, University of Michigan, using the words "breast" and "cancer" and "breast" and "carcinoma" from years 1987-1991. We identified 385 consecutive invasive breast cancer patients. Of the 385 cases, 236 cases were available for study. The reasons for this were: 1. unavailability of tissue slides or blocks, and 2. primary resection performed at a referring institution.

b. Histopathologic study of the cases and selection of adequate tumor areas to construct the tissue microarrays. Categorize the breast cancers according to stage.
The P.I. reviewed all the hematoxylin and eosin stained sections from all these cases and annotated the pathologic characteristics of each tumor using the following template:

Summary for Invasive Carcinomas.

Greatest dimension of invasive carcinoma (microscopic):						**cm**
Involvement of surgical margin:		**Positive (at ink)**				**Close (<= 0.2 cm)**
		Negative (>0.2 cm)				
If margin positive:			**Single focus**			**Multiple foci**
If margin close:			**Single focus**			**Multiple foci**
Histopathological grade (Elton and Ellis):			**1**	**2**	**3**	
Positive lymph nodes /total lymph nodes:				/		
Highest axillary node positive:			**Yes**		**No**	**N/A**
Extranodal extension:			**Yes**		**No**	**N/A**
Extensive DCIS:			**Yes**		**No**	**N/A**
DCIS > 25% of tumor:			**Yes**		**No**	
Extratumoral DCIS:			**Yes**		**No**	
Microcalcifications:	**None**		**within inv/DCIS**			**within benign ducts**
Hormonal receptors:	ER:	**POS**	**NEG**		PR:	**POS** **NEG**
Her2neu overexpression:		**POS**	**(2+**	**3+)**	**NEG**	
T	**N**	**M**				

Development of a breast cancer database
We developed a relational database in Microsoft Access to store the pathological and clinical information. The idea behind this decision was to be able to link the results of the TMA scoring with the patient pathological and clinical information. Clinical and treatment information was extracted by chart review, performed with IRB approval. The P.I. was involved in all steps of the database design and development, and learned how to perform database queries.

c. Construction of the tissue microarrays
We have constructed four high density tissue microarrays (TMAs) that will enable us to characterize WISP3 and RhoC expression in a wide range of normal breast and breast disease, and to study associations between expression of these proteins and patient outcome. The figure below is a schematic representation of a TMA.

In order to construct the tissue arrays, the P.I. reviewed all cases histologically and selected the areas to array. At least three different areas of the tumors were selected and at least three tissue cores (0.6 mm in diameter) were sampled from each donor block. TMAs are assembled using the manual tissue puncher/array (Beecher Instruments). This instrument consists of thin-walled stainless steel needles with an inner diameter of approximately 600 μm and stylet used to transfer and empty the needle contents. The assembly is held in an X-Y position guide that is manually adjusted by digital micrometers. Small biopsies are retrieved from selected regions of donor tissue and are precisely arrayed in a new paraffin block. Cores are inserted into a 45 x 20 x 12 mm recipient block and spaced at a distance of 0.8 mm apart.

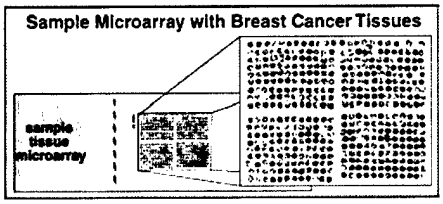

Figure 1.

d. Immunohistochemical analysis for RhoC-GTPase and WISP3 proteins, and other markers (ER, PR, HER2/neu, Ki-67, microvessel density and apoptosis).

We have optimized the conditions for immunohistochemistry for the anti-RhoC antibody and applied it to the constructed TMAs successfully. We used 1:400 dilution of antibody incubated overnight, and microwave antigen retrieval. Below are examples of tissues stained using RhoC antibody:

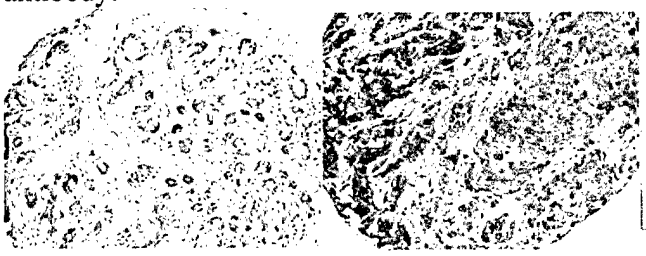

Figure 2. Examples of a tissue microarray element with a hyperplastic benign breast lobule staining weakly for RhoC (left), and an invasive carcinoma, staining strongly for RhoC (right).

We have worked closely with Covance in developing two antigenic peptides and immunizing rabbits to obtain polyclonal antibodies against WISP3. The following peptides were synthesized and polyclonal antibodies were obtained:
Ac-CSGAKGGKKDSDQSN-CONH2
Ac-CPEGRPGEVSDAPQRKQ-CONH2.

After evaluating 4 different anti-WISP3 antibodies, we selected the one that worked better for Western blot and gave a specific band (shown below).

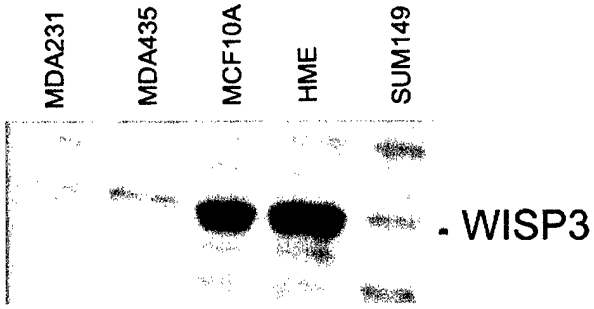

Figure 3. Western immunoblot of cell lysates of five different breast cancer cell lines (MDA231, MDA435, SUM149), and HPV immortalized human mammary epithelial cells (HME), and spontaneously immortalized human mammary epithelial cells (MCF10A). WISP3 protein is expressed in normal cells, and its expression decreases in breast cancer cells.

We have optimized the conditions for the anti-WISP3 antibody for immunohistochemistry and we have applied it to the TMAs successfully. We use the antibody at 1:100 dilution, with 60 minutes incubation and microwave antigen retrieval. Below are examples of the tissues microarray samples stained with anti-WISP3 antibody. We have also stained the TMAs for estrogen receptor, progesterone receptor and HER-2/neu.

e. Interpretation and grading of the immunohistochemical studies and statistical analyses.
I evaluated the immunohistochemistry for RhoC, ER, PR and HER-2/neu in all the TMAs, and with the assistance of Kent Griffith, the biostatistician, have analyzed the results which are shown below. I am in the process of evaluating the immunohistochemistry for WISP3, to explore its clinical relevance.
Below is the summary of our RhoC analyses, which are the subject of a manuscript that is ready for submission (see appendix).

We found that RhoC expression increases with breast cancer progression. All samples of normal breast epithelium had negative to weak staining, whereas staining intensity increased in hyperplasia, DCIS, invasive carcinoma, and metastases (Kruskal-Wallis $p<0.001$) Figure 5.

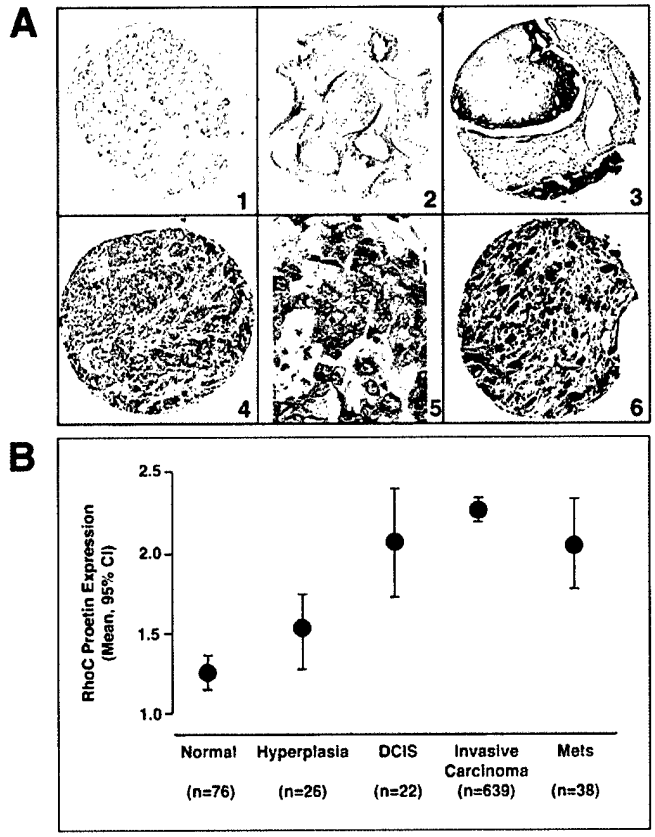

Figure 4. **RhoC protein expression increases with breast cancer progression. A.** tissue microarray samples of a normal breast lobule (1) and intraductal hyperplasia (2) with negative and weak RhoC expression. Ductal carcinoma *in situ* with comedo-necrosis (3) and invasive ductal carcinoma (4) with moderate and high RhoC expression, respectively. High power magnification of an invasive ductal carcinoma showing cytoplasmic accumulation of RhoC protein (5). Metastatic breast carcinoma in bone (6) with high expression of RhoC. **B.** Mean RhoC expression increases with the severity of the diagnosis. Original magnification 40x, and 100x.

The following table shows the clinicopathologic features for the patients with invasive carcinoma

Characteristics	*N (%)*[†]
Tumor size (cm) (N = 212)	
≤ 2	121 (57.1)
>2	91 (42.9)
Lymph nodes (N = 200)	
All negative	104 (52.0)
At least one positive	96 (48.0)
1-3 positive nodes	49 (24.5)
> 4 positive nodes	47 (23.5)
Tumor stage (N = 209)	
I	79 (37.8)
II	80 (38.3)
III	46 (22.0)
IV	4 (1.9)
Tumor grade (N = 212)	
I	25 (11.8)
II	103 (48.6)
III	84 (39.6)
Surgical margins (N = 211)	
Negative	147 (69.7)
Positive	35 (16.6)
Close (< 2 mm)	29 (13.7)
Angiolymphatic invasion (N = 233)	
Present	69 (29.6)
Absent	164 (70.4)
Estrogen receptor (N = 227)	
Positive	154 (67.8)
Negative	73 (32.2)
Progesterone receptor (N = 227)	
Positive	129 (56.8)
Negative	98 (43.2)
Her2/Neu (N = 226)	
Positive	41 (18.1)
Negative	184 (81.9)

RhoC expression was associated with negative ER expression and worse histologic grade. The table below show the associations between RhoC expression and clinical and pathologic features.

Characteristic	*Odds Ratio*	*95% CI*	*p-value*
Tumor size (cm) (N=212)			
≤ 2	1.00		
>2	1.30	0.78 – 2.16	0.3133
Tumor grade (N=213)			
I	1.00		
II	3.33	1.43 – 7.72	0.0051
III	6.19	2.58 – 14.85	<0.0001
Positive lymph nodes (N=201)			
0	1.00		

1-3	1.64	0.87 – 3.07	0.1237
4 or more	1.47	0.78 – 2.78	0.2340
Angiolymphatic invasion (N=233)			
Absent	1.00		
Present	1.19	0.71 – 2.00	0.5180
Estrogen receptor (N=228)			
Positive	1.00		
Negative	1.67	0.99 – 2.81	0.0510
Progesterone receptor (N=228)			
Positive	1.00		
Negative	2.32	1.41 – 3.82	0.0009
Her2/Neu expression (N=226)			
Negative	1.00		
Positive	1.86	0.99 – 3.48	0.0558

In patients with invasive carcinoma, high RhoC expression was an independent predictor of death from breast cancer, and of local-recurrence free survival. The hazard ratio for local recurrence for patients with high RhoC levels as compared with those with low RhoC levels was 2.37, with a 95% confidence interval of 1.18-4.77 (p=0.015).

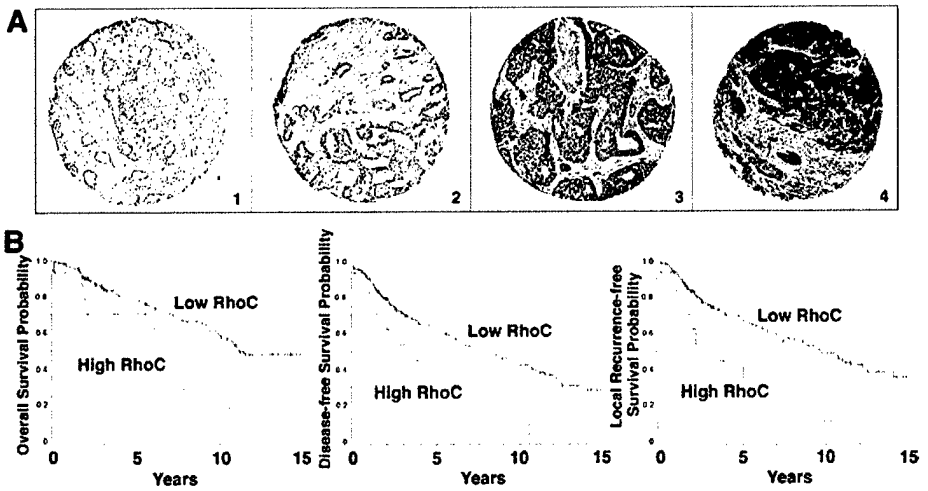

Figure 5. **RhoC protein expression is associated with survival in patients with breast cancer. A.** Tissue microarray elements containing representative invasive carcinomas with negative (1), weak (2), moderate (3), and strong (4) RhoC staining intensities. Original magnification 40x. **B.** High RhoC expression in invasive carcinomas is associated with worse overall, disease-free, and local recurrence-free survival.

Our preliminary studies show that RhoC expression increases with breast cancer progression and RhoC protein levels in tumor tissue, as measured by immunohistochemistry, are strongly associated with survival and local recurrence in patients with breast cancer.This not only extends our initial observations (Kleer et al, Am J Pathol 2002 Feb;160(2):579-84), but also suggests that RhoC may have a role in the local invasiveness and progression of breast carcinoma. Our studies suggest that RhoC protein levels may be first altered in carcinoma *in situ*, the precursor of

invasive carcinoma. Clinically, our retrospective study suggest that RhoC levels may prove useful after further validation, to identify patients with breast cancer that are likely to recur locally.

Task 2. To define the role of Rho-GTPase and WISP3 in the clinical setting as independent predictors of survival in patients with locally advanced breast cancer. Months 24-36.

a. Histopathologic study of 89 cases of locally advanced breast cancer that were previously retrieved from the pathology files (first 6 months). Selection of adequate areas to construct the tissue microarray. Months 24-27.
b. Development of the tissue microarray, and immunohistochemical analysis of RhoC-GTPase, WISP3 and other biomarkers (ER, PR, HER2/neu, Ki-67, microvessel density and apoptosis). Months 28-33.
c. Interpretation and grading of the immunohistochemical stains and statistical analyses. Months 33-36.

Task 2.

a. Histopathologic study of 89 cases of locally advanced breast cancer that were previously retrieved from the pathology files (first 6 months). Selection of adequate areas to construct the tissue microarray. Months 24-27.
So far, we have identified 60 cases of locally advanced breast cancer, of which 30 are inflammatory breast cancers, and 30 are stage matched, non-inflammatory breast cancer were identified from the pathology files. We evaluated them histologically and chose the areas to construct a TMA
d. Development of the tissue microarray, and immunohistochemical analysis of RhoC-GTPase, WISP3 and other biomarkers (ER, PR, HER2/neu, Ki-67, microvessel density and apoptosis). Months 28-33.
We have constructed a TMA with these tissues, and stained them for RhoC, ER, PR and HER-2/neu. We have stained the TMA for WISP3 as well and are in the process of evaluating the immunohistochemical results.
e. Interpretation and grading of the immunohistochemical stains and statistical analyses. Months 33-36.
RhoC, ER, PR and Her-2/neu stains have been evaluated and analyzed in conjunction with Task 1. We are in the process of interpreting the immunohistochemical results for WISP3 staining in this group as well. Once this is performed, we will analyze the value of RhoC and WISP3 expression in predicting response to therapy in this group of tumors.

Task 3. To study in detail the *in vivo* effect of WISP3 loss in modulating the response of invasive breast carcinomas with RhoC-GTPase over-expression to farnesyl transferase inhibitors. Months 36-48.

a. Prepare a panel of cell lines (SUM149 wt, SUM149/WISP3, HME/RhoC, SUM185 wt and MCF10AT wt). Since all these cell lines have been prepared in our preliminary work, getting them ready for injection with take approximately 3 weeks. Month 36-37.
b. In vivo mice experiment (injection of cell lines, tumor development and treatment with farnesyl transferase inhibitor). Months 38-41.

c. Histological and immunohistochemical study of the excised tumors stained with anti-RhoC and anti-WISP3 antibodies. Months 42-44.
d. Analysis of the immunostains. Months 44-46.
e. Statistical analyses. Months 46-48.

We have not yet initiated the experiments in Task 2. They will commence this year.

In addition to the Tasks, we have performed seminal work in understanding WISP3 function, and how WISP3 and RhoC may cooperate to determine a highly aggressive inflammatory breast cancer phenotype, which we have published (Kleer et al, WISP3 and RhoC guanosine triphosphatase cooperate in the development of inflammatory breast cancer. Breast Cancer Res. 2004;6(1):R110-5). In this work, we found that antisense inhibition of WISP3 in HME cells increased RhoC mRNA and resulted in an increase in cellular proliferation, anchorage independent growth and VEGF levels in the conditioned media. Conversely, restoration of WISP3 expression in the highly malignant IBC cell line, SUM149, was able to decrease the expression of RhoC protein.

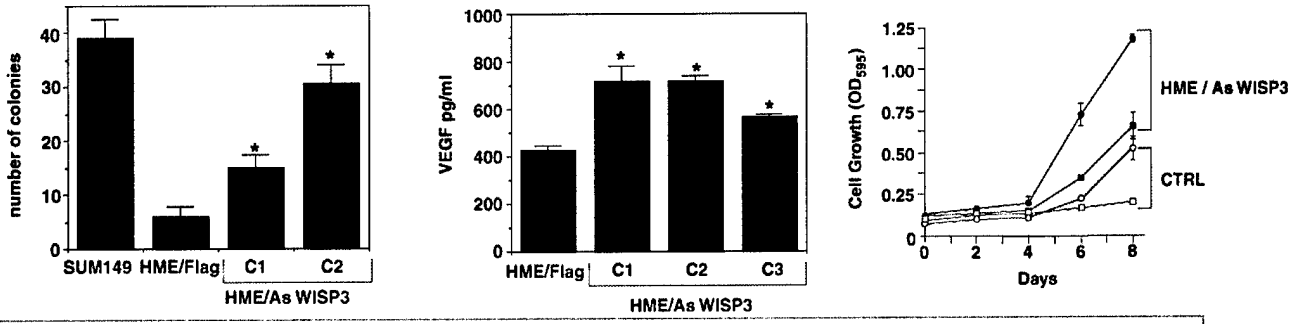

Figure 6. **Inhibition of WISP3 induces anchorage-independent growth, proliferation and secretion of VEGF in HME cells.** (A) Inhibition of WISP3 expression in HME cells HME cells greatly increased the number of colonies formed in soft agar when compared to empty vector control (HME/ Flag) t test, $p<0.05$ for both clones. (B) Effect of inhibition of WISP3 expression on the proliferation of HME cells was studied with the MTT assay. The stable HME/ AS WISP3 cells have a significant increase in the proliferation rate when compared to the empty vector control. Results are expressed as mean ± SEM of three independent experiments. 3,000 cells were assessed in each plate (t test, $p<0.05$). (C) Increase in VEGF measured by ELISA, as a result of inhibition of WISP3 expression in HME cells. Results are expressed as mean ± SEM, t test $p<0.05$ for all clones.

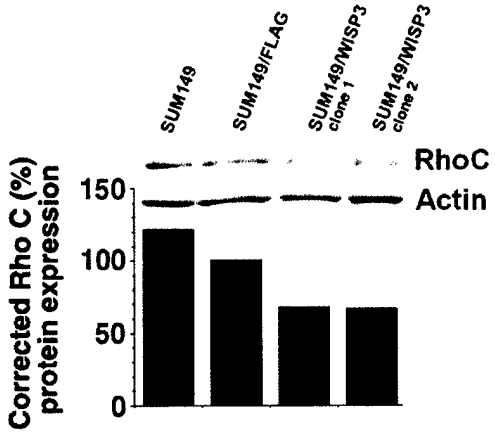

Figure 7. **Restoration of WISP3 expression in SUM149 inflammatory breast cancer cells decreases RhoC protein expression.** Western immunoblot of cell culture of SUM 149 cells, empty vector control (SUM149/ Flag), and two WISP3 expressing clones using antibodies for RhoC and actin. Gels were scanned and pixel intensity values were obtained. Values for RhoC were corrected for loading by dividing the RhoC pixel intensity by the actin pixel intensity.

In summary, WISP3 modulates RhoC expression in HME cells and in the IBC cell line SUM149. This provides further evidence in support that these two genes act in concert to give rise to the highly aggressive IBC phenotype. We propose a model of this interaction as a starting point for further investigations. This manuscript is included in the appendix.

We have also made an important contribution by elucidating that WISP3 is a secreted protein and that it modulates IGF signaling. This work is seminal, as no other tumor suppressor gene has ever been defined specifically for Inflammatory Breast Cancer. Previoulsy, we have demonstrated that WISP3 has tumor suppressor functions in IBC (Kleer et al, *Oncogene*, 21, 3172-3180, 2002), and we have gained insight into WISP3 as a modulator of IGF signaling. This work was presented at the AACR meeting in Washington DC, July, 2003 as an oral presentation, and has been recently published in *Neoplasia* and is included in the appendix. (Kleer et al, Neoplasia 2004 Mar-Apr;6(2):179-85).

In this work, we found that WISP3 is secreted into the conditioned media and into the lumens of normal breast ducts. Once secreted, WISP3 was able to decrease, directly or through induction of other molecule(s), the IGF-1-induced activation of the IGF-IR, and two of its main downstream signaling molecules, IRS1 and ERK-1/2 in SUM149 IBC cells. Furthermore, WISP3 containing conditioned media decreased the growth rate of SUM149 cells. This work sheds light into the mechanism of WISP3 function by demonstrating that it is secreted, and that once in the extracellular media it induces a series of molecular events that lead to modulation of IGF-IR signaling pathways and cellular growth in IBC cells.

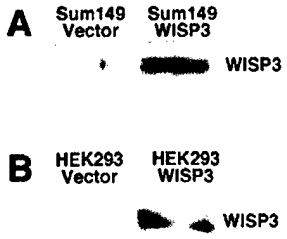

Figure 8. **WISP3 protein is secreted and detected in the conditioned media. A** Western immunoblot using anti-WISP3 polyclonal antibody detects WISP3 protein in the conditioned media of SUM149 cells transfected with WISP3 full-length cDNA. **B** Western immunoblot of the conditioned media of HEK-293 cells transfected with WISP3, detected using an anti-HIS antibody. WISP3 is not detected in the conditioned media of the control cells.

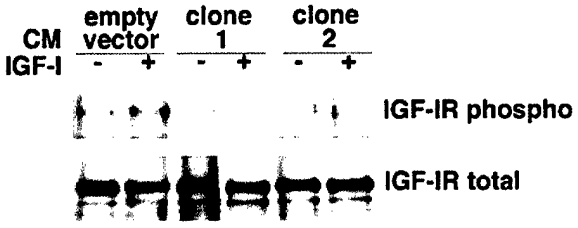

Figure 9. **WISP3 decreases IGF-I-induced phosphorylation of the IGF-IR.** Western blot of SUM149 cell lines bathed in WISP3+ and control (WISP3-) conditioned media. The experiment was carried out under baseline conditions (without IGF-I) and after stimulation with 20 ng/ml of IGF-I. The IGF-IR was precipitated from 500 μg of protein lysate with an anti-IGF-IR mAb and subsequently detected by immunoblot with an anti-IGF-IR β subunit polyclonal Ab. Tyrosine phosphorylation of immunoprecipitated IGF-IR was assessed with an anti-phosphotyrosine mAb PY20.

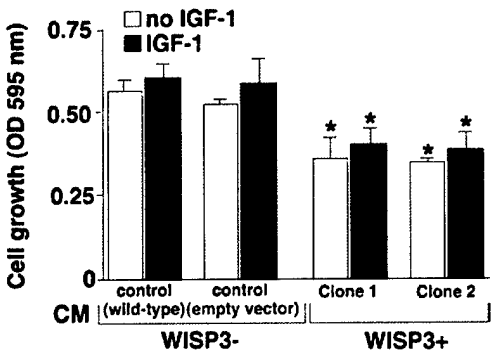

Figure 10. **WISP3 decreases the growth of IBC cells.** The growth of SUM149 cells was measured in the absence (WISP3-) and in the presence of WISP3 (WISP3+) in the conditioned media under baseline conditions (no IGF-I) and after IGF-I stimulation, by an MTT assay. SUM149 cells were grown in 96-well plates at a density of 5 x 104 cells/ml. Serum starved cells were incubated for 24 hours in the WISP3 and control conditioned media, with or without IGF-I stimulation. Results are expressed as mean ± SEM of three independent experiments. WISP3 + conditioned media decreases significantly the growth of SUM149 cells (t test, $p<0.05$ for both clones).

We have also identified that EZH2 is a marker of aggressive breast cancer and that it promotes the neoplastic transformation of human mammary epithelial cells (Kleer CG, Cao Q, Varambally S, Shen R, Ota I, Tomlins SA, Ghosh D, Sewalt, RG, Otte AP, Hayes DF, Sabel MS, Livant D, Weiss SJ, Rubin MA and Chinnaiyan AM. EZH2 is a Marker of Aggressive Breast Cancer and Promotes Neoplastic Transformation of Breast Epithelial Cells. *Proceedings of the National Academy of Sciences*, 100(20): 11606-11, 2003). For this study, we used the tissue microarrays constructed and stained them using a polyclonal antibody for EZH2, a transcriptional repressor. We found that EZH2 expression was an independent factor that predicts death from breast cancer. We have included a copy reprint of this paper in the appendix section.

In summary, we have had a very productive year where we have completed several manuscripts dealing with key aspects of WISP3 and RhoC expression in breast cancer. We have developed key reagents and resources that will enable us to move forward in testing their clinical usefulness. We have also completed a major effort in understanding the function of WISP3 gene as it contributes to the inflammatory breast cancer phenotype.

Key Research Accomplishments so far

- Constructed four high density tissue microarrays
- Developed a relational database with the patient information
- Generated and tested a polyclonal antibody against WISP3
- Validation of RhoC as a novel tissue biomarker that predicts local recurrence and survival in patients with breast cancer.
- Investigated the mechanisms of cooperation between RhoC and WISP3 in determining the inflammatory breast cancer phenotype.
- Elucidated that WISP3 is a secreted protein and that it modulates IGF-I signaling cascade in inflammatory breast cancer
- Discovered that EZH2 is a marker of aggressive breast cancer and that it promotes neoplastic transformation of mammary epithelial cells.

Training component of the Award
During this year, the P.I. has had a significant learning opportunity was to direct and work closely with the statistician to perform survival analyses for RhoC, and for EZH2.
In the laboratory, the P.I. learned how to design and interpret the experiment conducted that revealed that WISP3 modulates IGF signaling pathways.
In developing the anti-WISP3 antibody, the P.I. learned how to design a peptide, and how to test and interpret the antibody at different points of the immune response.

Reportable Outcomes
We are in a position to report that RhoC over expression is an early marker of aggressive breast cancers, even when they are small, and that it is a promising marker of prognosis and local recurrence in patients with breast cancer.
We can state that WISP3 is able to ameliorate the highly malignant features of inflammatory breast cancer. Specifically, WISP3 has growth and angiogenic inhibitory functions, at least in part though modulating IGF-receptor signaling pathways.
We can state that EZH2 is a marker of aggressive breast cancer, and that it can predict prognosis.

Research Manuscripts published for the period 17 April 2003- 16 April 2004:

Kleer CG, Cao Q, Varambally S, Shen R, Ota I, Tomlins SA, Ghosh D, Sewalt RG, Otte AP, Hayes DF, Sabel MS, Livant D, Weiss SJ, Rubin MA and Chinnaiyan AM. EZH2 is a Marker of Aggressive Breast Cancer and Promotes Neoplastic Transformation of Breast Epithelial Cells. *Proceedings of the National Academy of Sciences,* 100(20):11606-11, 2003.

Kowalski PJ, Rubin MA and Kleer CG. E-Cadherin Expression in Primary Carcinomas of the Breast and its Distant Metastases. *Breast Cancer Research*, 5:R217-R222, 2003.

Kleer CG, Zhang Y, Pan Q, Wolf J, Wu M, Wu Z-F, Merajver SD. WISP3 and RhoC-GTPase Cooperate in the Development of Inflammatory Breast Cancer. *Breast Cancer Research* 6(1): R110-5, 2004.

Ray ME, Yang ZQ, Albertson D, Kleer CG, Washburn JG, Macoska JA, Ethier SP. Genomic and Expression Analysis of the 8p11-12 Amplicon in Human Breast Cancer Cell Lines. *Cancer Research* 64(1):40-47, 2004.

Van Den Eynden GG, Van Der Auwera I, Van Laere S, Colpaert CG, Van Dam P, Merajver S, Kleer CG, Harris AL, Van Marck EA, Dirix LY, Vermeulen PB. Validation of a tissue microarray to study differential protein expression in inflammatory and non-inflammatory breast cancer. *Breast Cancer Res Treat.* 85(1):13-22, 2004.

Kleer CG, Zhang Y, Pan Q, Merajver SD. WISP3 is a Secreted Tumor Suppressor Protein that Modulates IGF Signaling in Inflammatory Breast Cancer. *Neoplasia,* 2004 Mar-Apr;6(2):179-85.

Abstracts:

Kleer CG, Zhang Y, Pan Q, Merajver SD. WISP3 is a secreted protein and modulates IGF signaling in inflammatory breast cancer. Minisymposium AACR Meeting, Washington DC, July 11-14, 2003.

Koker M and Kleer CG. Metaplastic Carcinoma of the Breast: P63 is a highly sensitive and specific marker. Platform Presentation, USCAP Meeting, Vancouver, BC, 2004.

Koker M, and Kleer CG. Smooth muscle actin and p63 in the diagnosis of difficult lesions of the breast. Poster Presentation, USCAP Meeting, Vancouver, BC, 2004.

Koker, M., Griffith K, Newman L, Sabel M, Rubin MA and Kleer CG. Pathologic Factors Predictive of Sentinel Lymph Node Metastasis in Patients with Breast Cancer. Poster Presentation, USCAP Meeting, Vancouver, BC, 2004.

Witniewski A, Rubin MA and Kleer CG. AMACR Expression in Breast Adenocarcinomas. Poster Presentation, USCAP Meeting, Vancouver, BC, 2004.

Kleer CG, Cao Q, Varambally S, Shen R, Ota I, Tomlins SA, Ghosh D, Sewalt RG, Otte AP, Hayes DF, Sabel MS, Livant D, Weiss SJ, Rubin MA and Chinnaiyan AM. EZH2 is a Marker of Aggressive Breast Cancer and Promotes Neoplastic Transformation of Breast Epithelial Cells. Platform Presentation, USCAP Meeting, Vancouver, BC, 2004.

Kleer CG, Griffith K, Sabel S, Gallagher G, Merajver SD. RhoC GTPase is a New Tissue Biomarker Predictive of Local Recurrence in Patients with Breast Cancer. Poster Presentation, AACR meeting, Orlando, FL, 2004.

Conclusion

We are encouraged by our progress. We want to move forward and test the clinical utility of WISP3 and in combination with RhoC and other markers, in detecting aggressive breast cancer phenotypes before they develop metastases. We also wish to explore the relationship between WISP3 and the IGF-receptor pathway in more depth. These are the directions we are moving on for this year.

References:

Manley, S., Mucci, N.R., De Marzo, A.M. & Rubin, M.A. Relational database structure to manage high-density tissue microarray data and images for pathology studies focusing on clinical outcome: the prostate specialized program of research excellence model. *Am J Pathol* 159, 837-43, 2001

Kleer CG, Zhang Y, Pan Q, van Golen KL, Wu Z-F, and Merajver SD. WISP3 Is a Novel Tumor Suppressor Gene of Inflammatory Breast Cancer. *Oncogene* 21, 3172-3180, 2002.

Kleer CG, van Golen KL, Zhang Y, Wu Z-F, Rubin MA, Merajver SD.

Characterization of RhoC Expression in Benign and Malignant Breast Disease: A Potential New Marker for Small Breast Carcinomas with Metastatic Potential. *Am J of Pathol.* 160(2), 579-584, 2002.

Valdez R, Thorson J, Finn WG, Schnitzer B, and Kleer CG. Lymphocytic Mastitis/ Diabetic Mastopathy: A Molecular, Immunophenotypic, and Clinicopathologic Evaluation of Eleven Cases. *Modern Pathology* 16: 223-228, 2003.

Kleer CG, Cao Q, Varambally S, Shen R, Ota I, Tomlins SA, Ghosh D, Sewalt RG, Otte AP, Hayes DF, Sabel MS, Livant D, Weiss SJ, Rubin MA and Chinnaiyan AM. EZH2 is a Marker of Aggressive Breast Cancer and Promotes Neoplastic Transformation of Breast Epithelial Cells. *Proceedings of the National Academy of Sciences,* 100(20):11606-11, 2003.

Kowalski PJ, Rubin MA and Kleer CG. E-Cadherin Expression in Primary Carcinomas of the Breast and its Distant Metastases. *Breast Cancer Research,* 5:R217-R222, 2003.

Kleer CG, Zhang Y, Pan Q, Wolf J, Wu M, Wu Z-F, Merajver SD. WISP3 and RhoC-GTPase Cooperate in the Development of Inflammatory Breast Cancer. *Breast Cancer Research* 6(1): R110-5, 2004.

Ray ME, Yang ZQ, Albertson D, Kleer CG, Washburn JG, Macoska JA, Ethier SP. Genomic and Expression Analysis of the 8p11-12 Amplicon in Human Breast Cancer Cell Lines. *Cancer Research* 64(1):40-47, 2004.

Van Den Eynden GG, Van Der Auwera I, Van Laere S, Colpaert CG, Van Dam P, Merajver S, Kleer CG, Harris AL, Van Marck EA, Dirix LY, Vermeulen PB. Validation of a tissue microarray to study differential protein expression in inflammatory and non-inflammatory breast cancer. *Breast Cancer Res Treat.* 85(1):13-22, 2004.

Kleer CG, Zhang Y, Pan Q, Merajver SD. WISP3 is a Secreted Tumor Suppressor Protein that Modulates IGF Signaling in Inflammatory Breast Cancer. *Neoplasia,* 2004 Mar-Apr;6(2):179-85.

Appendix

Research article

Open Access

WISP3 and RhoC guanosine triphosphatase cooperate in the development of inflammatory breast cancer

Celina G Kleer[1,3], Yanhong Zhang[1,3], Quintin Pan[2,3], Gary Gallagher[1,3], Mei Wu[1,2], Zhi-Fen Wu[2,3] and Sofia D Merajver[2,3]

[1]Department of Pathology, Univeristy of Michigan, Ann Arbor, MI, USA
[2]Department of Internal Medicine, Univeristy of Michigan, Ann Arbor, MI, USA
[3]Comprehensive Cancer Center, Univeristy of Michigan, Ann Arbor, MI, USA

Correspondence: Sofia D Merajver (e-mail: smerajve@umich.edu)

Received: 17 Jun 2003 Revisions requested: 28 Aug 2003 Revisions received: 4 Dec 2003 Accepted: 5 Dec 2003 Published: 19 Dec 2003

Breast Cancer Res 2004, **6**:R110-R115 (DOI 10.1186/bcr755)

Abstract

Background: Inflammatory breast cancer (IBC) is the most lethal form of locally advanced breast cancer. We found concordant and consistent alterations of two genes in 90% of IBC tumors when compared with stage-matched non-IBC tumors: overexpression of RhoC guanosine triphosphatase and loss of WNT-1 induced secreted protein 3 (WISP3). Further work revealed that RhoC is a transforming oncogene for human mammary epithelial (HME) cells. Despite the aggressiveness of the RhoC-driven phenotype, it does not quantitatively reach that of the true IBC tumors. We have demonstrated that WISP3 has tumor growth and angiogenesis inhibitory functions in IBC. We proposed that RhoC and WISP3 cooperate in the development of IBC.

Methods: Using an antisense approach, we blocked WISP3 expression in HME cells. Cellular proliferation and growth were determined using the 3-[4,5-dimethylthiazol-2-yl]-2,5-diphenyltetrazolium bromide (MTT) assay and anchorage-independent growth in a soft agar assay. Vascular endothelial growth factor (VEGF) was measured in conditioned medium by enzyme-linked immunosorbent assay.

Results: Antisense inhibition of WISP3 in HME cells increased RhoC mRNA levels and resulted in an increase in cellular proliferation, anchorage-independent growth and VEGF levels in the conditioned medium. Conversely, restoration of WISP3 expression in the highly malignant IBC cell line SUM149 was able to decrease the expression of RhoC protein.

Conclusion: WISP3 modulates RhoC expression in HME cells and in the IBC cell line SUM149. This provides further evidence that these two genes act in concert to give rise to the highly aggressive IBC phenotype. We propose a model of this interaction as a starting point for further investigations.

Keywords: CCN proteins, motility, oncogene, tumor suppressor gene, vascular endothelial growth factor, WNT-pathway

Introduction

Inflammatory breast cancer (IBC) is the most lethal form of locally advanced breast cancer and accounts for approximately 6% of new breast cancer cases annually in the United States [1,2]. IBC has distinct clinical and pathological features. Patients present with erythema, skin nodules, dimpling of the skin (termed 'peau d'orange'), all features that develop rapidly, typically progressing within 6 months [1–4]. One salient feature of IBC that is observed in tissue sections is that cancer cells form emboli that spread through the dermal lymphatics. The dermatotropism of IBC is believed to be responsible for the clinical signs and symptoms and probably enables effective dissemination to distant sites [2]. These observations lead us to conclude that IBC is highly invasive and that it is capable of metastases from its inception. Indeed, at the time of diagnosis, most patients have locoregional and/or distant metastatic disease [3,4]. In spite of new advances in breast cancer

FBS = fetal bovine serum; GTPase = guanosine triphosphatase; HME = human mammary epithelial; IBC = inflammatory breast cancer; MTT = 3-[4,5-dimethylthiazol-2-yl]-2,5-diphenyltetrazolium bromide; PCR = polymerase chain reaction; RT–PCR = reverse transcriptase PCR; VEGF = vascular endothelial growth factor; WISP3 = WNT-1 induced secreted protein 3.

therapy including multimodality approaches, the 5-year disease-free survival rate is less than 45% [3,4].

Until recently, no biological markers defined the IBC phenotype. We proposed that a limited number of genetic alterations, occurring in rapid succession or concordantly, are responsible for the rapidly progressive and distinct clinical and pathological features of IBC. Using a modified version of the differential display technique and *in situ* hybridization of human tumors, we identified two genes that are consistently and concordantly altered in human IBC when compared with stage-matched non-IBC tumors: loss of WISP3 and overexpression of RhoC guanosine triphosphatase (GTPase) [5].

WNT-1 induced secreted protein 3 (WISP3) is a member of the CCN family of proteins, which have important biological functions in normal physiology as well as in carcinogenesis [6–8]. We found that WISP3 has growth and angiogenesis inhibitory functions in IBC *in vitro* and *in vivo* [9]. RhoC GTPase is a member of the Ras superfamily of small GTPases. Activation of Rho proteins leads to assembly of the actin–myosin contractile filaments into focal adhesion complexes that bring about cell polarity and facilitate motility [10–12]. Our laboratory has characterized RhoC as a transforming oncogene for human mammary epithelial (HME) cells; its overexpression results in a highly motile and invasive phenotype that recapitulates the IBC phenotype. Predicated on the high rate of concordance of RhoC and WISP3 changes in IBC, we propose that these two genes cooperate to determine this highly metastatic, unique breast cancer phenotype.

Materials and methods

Cell culture

The derivation of the SUM149 cell line has been described previously by Ethier et al [13]. This cell line was developed from a human primary IBC and has lost WISP3 expression [9]. HME cells were immortalized with human papilloma virus E6/E7 and were characterized as being keratin 19 positive, ensuring that they are from the same differentiation lineage as the SUM149 IBC tumor cell line [14,15]. MCF10A cells are spontaneously immortalized human mammary epithelial cells. Cells were cultured in Ham's F-12 medium supplemented with 5% fetal bovine serum (FBS), hydrocortisone (1 μg/ml), insulin (5 μg/ml), fungizone (2.5 μg/ml), gentamycin (5 μg/ml), penicillin (100 U/ml) and streptomycin (10 μg/ml) at 37°C under 10% CO_2.

Construction of expression vectors and stable transfections

Total RNAs were isolated from HME cells with a Trizol kit (Life Technologies, Inc, Gaithersburg, MD). First-strand cDNA synthesis was performed by using 1 μg of total RNA with AMV reverse transcriptase (Promega, Madison, WI) and oligo(dT) as a primer. A 2 μl portion of the reaction mixture was used for amplification by polymerase chain reaction (PCR). Human WISP3 cDNA was amplified by PCR with the forward and reverse primers 5′-ACGAATTCAATGAACAAGCGGCG-3′ and 3′-GCGAATTCTTTTACAGAATCTTG-5′, respectively, under the following conditions: denaturing for 1 min at 94°C, annealing for 1 min at 58°C, and elongation for 1 min at 72°C, for 35 cycles. PCR products were cloned into pGEM-T Easy vector (Promega). The 1.1 kb full-length cDNA encoding WISP3 was excised by *Eco*RI and subcloned into the *Eco*RI site of pFlag-CMV4 vector (Sigma, St Louis, MO). The insert was confirmed by DNA sequencing. The plasmids were purified. Subsequently, the SUM149 cells were transfected with pFlag-WISP3 sense (SUM149/WISP3), and HME cells were transfected with pFlag-WISP3 antisense (HME/AS WISP3). MCF10A cells were stably tranfected with full-length RhoC cDNA (MCF10A/RhoC). pFlag control vectors were used as controls (FuGene TM 6 transfection reagent; Roch–Boehringer-Mannheim, Germany). Transfectants were selected in the medium containing 150 μg/ml G418. The cells surviving during selection were expanded and maintained in the selected medium.

Reverse transcriptase PCR (RT–PCR) analysis

Total RNA (1 μg) from HME/AS WISP3 clones and empty vector controls were reverse-transcribed with Superscript reverse transcriptase (Invitrogen) using oligo(dT) and random hexanucleotide primer for first-strand cDNA synthesis. PCRs were performed directly on 1 μl of first-strand cDNA using 500 nmol of each of the following gene-specific primers: WISP3, 5′-ATGCAGGGGCTCCTCTTCTGC-3′ (forward primer) and 5′-ACTTTTCCCCCATTTGCTTG-3′ (reverse primer); RhoC , 5′-ATGGCTGCAATCCGAAAG-3′ (forward primer) and 5′-GATCTCAGAGAATGGGACAGC-3′ (reverse primer); GAPDH, 5′-CGGAGTCAACGGATTTGGTCGTAT-3′ (forward primer) and 5′-AGCCTTCTCCATGGTGGTGAAGAC-3′ (reverse primer). The 100 μl reaction volume consisted of 50 mM KCl, 10 mM Tris-HCl pH 8.3, 1.5 mM $MgCl_2$, and deoxynucleotide triphosphates (each at 200 μM). PCR was performed for initial denaturation at 94°C for 5 min, followed by 35 cycles of denaturation (94°C, 1 min), annealing (55°C, 1 min), and extension (72°C, 1 min) with 5 units of *Taq* polymerase (Invitrogen). This was followed by a final extension step at 72°C for 10 min. The products were analyzed on 1% agarose gels stained with ethidium bromide and detected with ultraviolet illumination.

Western immunoblots

Western immunoblots were performed with polyclonal anti-RhoC and anti-WISP3 antibodies. Cultured cells were washed in ice-cold phosphate-buffered saline, lysed in lysis buffer (10% glycerol, 50 mM Tris-HCl pH 7.4, 100 mM NaCl, 1% Nonidet P40, 2 mM $MgCl_2$, 1 μg/ml leupeptin, 1 μg/ml aprotinin, 1 mM phenylmethylsulphonyl

fluoride) on ice for 5 min, and then centrifuged for 5 min at 4°C. Cleared lysates (each containing 50 μg of protein) were subjected to SDS–polyacrylamide-gel electrophoresis and transferred to poly(vinylidene difluoride) membrane. Western blots were performed as described previously, with anti-RhoC rabbit polyclonal antibody and anti-β-actin goat antibody (Sigma) at dilutions of 1 : 1500 and 1 : 2000, respectively [16].

Anchorage-independent growth

For studies of anchorage-independent growth we performed soft agar assays on stable clones of HME/AS WISP3, HME/Flag, and SUM149 cells. Each well of a six-well plate was first layered with 0.6% agar diluted with 10% FBS-supplemented Ham's F-12 medium complete with growth factors. The cell layer was then prepared by diluting agarose to concentrations of 0.3% and 0.6% with 10^3 cells in 2.5% FBS-supplemented Ham's F-12/1.5 ml/well. Plates were maintained at 37°C under 10% CO_2 for 3 weeks. Colonies 100 μm or more in diameter were counted under the microscope with a grid.

Monolayer growth rate

Monolayer culture growth rate was determined by qualitative measurement of the conversion of 3-(4,5-dimethylthiazol-2-yl)-2,5-diphenyltetrazolium bromide (MTT; Sigma) to a water-insoluble formazan by viable cells. In all, 3000 cells obtained for HME/AS WISP3 clones, HME/Flag, and HME wild-type cells, suspended in 200 μl of culture medium, were plated in 96-well plates and grown under normal conditions. Cultures were assayed at 0, 2, 4, 6, and 8 days by the addition of MTT and incubation for 1 hour at 37°C. The MTT-containing medium was aspirated and 100 μl of dimethyl sulphoxide (Sigma) was added to lyse the cells and solubilize the formazan. Optical densities of the lysates were determined on a Dynatech MR 5000 microplate reader at 595 nm.

Analysis of vascular endothelial growth factor

Conditioned medium was generated by incubating HME/AS WISP3 cells, HME/Flag cells, and SUM149 cells in serum-free medium. After 3 days the medium was collected, cleared of cell debris by centrifugation, concentrated approximately 10-fold through a Centriplus YM-10 column (Millipore, Bedford, MA). The levels of vascular endothelial growth factor (VEGF), which is a factor known to be secreted by IBC, were measured in the cell culture supernatants by enzyme-linked immunosorbent assay, as described previously [9,17].

Results

Inhibition of WISP3 increases RhoC mRNA levels in immortalized HME cells and induces proliferation, anchorage-independent growth, and VEGF production

To study the effects of inhibition of WISP3 expression on the phenotype of HME cells, we established clones of HME cells stably transfected with antisense WISP3 constructs (HME/AS WISP3). Effective inhibition of WISP3 expression was confirmed by RT–PCR (Fig. 1). Inhibition of WISP3 expression in HME cells resulted in increased expression of RhoC transcript in comparison with HME cells transfected with the control empty vector (Fig. 1). After 14 days of growth in soft agar, inhibition of WISP3 expression in HME cells resulted in a significant increase in the number of colonies formed in comparison with the empty vector control (*t*-test, $P<0.05$ for both clones; Fig. 2a). Inhibition of WISP3 expression resulted in an increase in cellular proliferation (*t*-test, $P<0.05$; Fig. 2b).

Figure 1

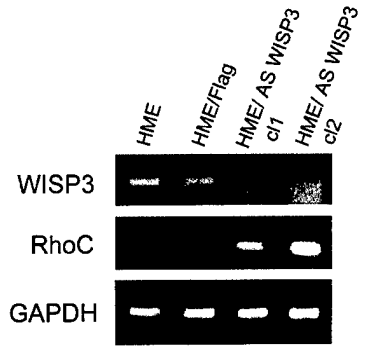

Inhibition of WISP3 in human mammary epithelial (HME) cells results in an increase in RhoC transcript levels. Reverse transcriptase polymerase chain reaction was conducted on vector and HME cells that have inhibition of WISP3 expression using full-length WISP3 antisense mRNA. HME/AS WISP3 cells showed increased levels of RhoC transcript in comparison with controls.

Previously, we had shown that restoration of WISP3 expression in an IBC cell line decreases the production of VEGF, a major pro-angiogenic factor secreted by IBC [9]. To determine the effect of WISP3 inhibition on the secretion of VEGF, we measured the concentration of VEGF in the conditioned medium of the stably transfected HME/AS WISP3 cells. Figure 2c shows that inhibition of WISP3 expression resulted in increased levels of VEGF in the conditioned medium (*t*-test, $P<0.05$ for all clones).

Restoration of WISP3 expression in SUM149 cells decreases RhoC expression

Because decreased expression of WISP3 in HME cells induced a significant increase in RhoC expression and some features of RhoC induced functional changes including anchorage-independent growth and production of VEGF, we sought to determine whether restoration of WISP3 expression in the SUM149 IBC cell line, which has lost WISP3 expression in the wild type, has an effect in RhoC expression. To test this, we stably transfected WISP3 in SUM149 cells and measured RhoC expression

Figure 2

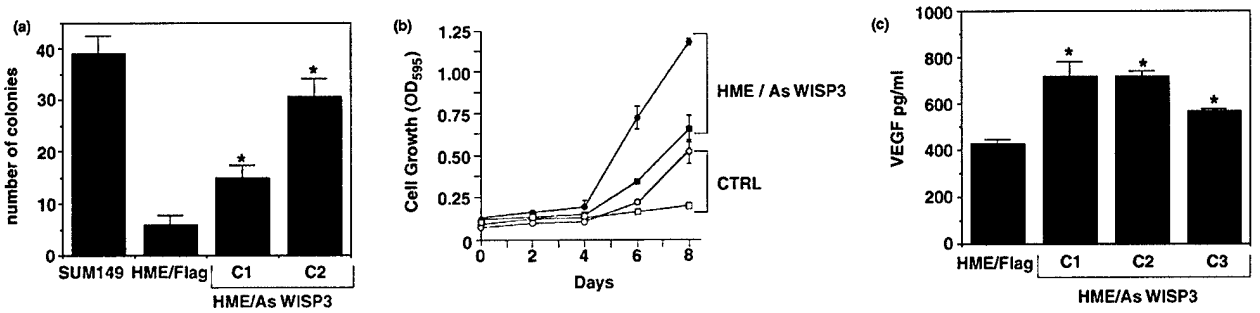

Inhibition of WISP3 induces anchorage-independent growth, proliferation and secretion of vascular endothelial growth factor (VEGF) in human mammary epithelial (HME) cells. **(a)** Inhibition of WISP3 expression in HME cells. HME cells greatly increased the number of colonies formed in soft agar in comparison with empty vector control (HME/Flag; *t*-test, $P<0.05$ for both clones). **(b)** Effect of inhibition of WISP3 expression on the proliferation of HME cells was studied with the 3-(4,5-dimethylthiazol-2-yl)-2,5-diphenyltetrazolium bromide (MTT) assay. The stable HME/AS WISP3 cells have a significant increase in the proliferation rate in comparison with the empty vector control. Results are expressed as means ± SEM of three independent experiments. In all, 3000 cells were assessed in each plate (*t*-test, $P<0.05$). **(c)** Increase in VEGF measured by enzyme-linked immunosorbent assay, as a result of inhibition of WISP3 expression in HME cells. Results are expressed as means ± SEM; *t*-test, $P<0.05$ for all clones.

Figure 3

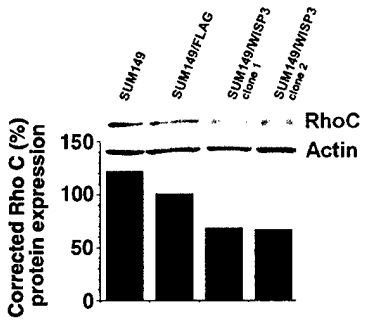

Restoration of WISP3 expression in SUM149 inflammatory breast cancer cells decreases RhoC protein expression. Western immunoblot of cell culture of SUM 149 cells, empty vector control (SUM149/Flag), and two WISP3-expressing clones with antibodies against RhoC and actin. Gels were scanned and pixel intensity values were obtained. Values for RhoC were corrected for loading by dividing the RhoC pixel intensity by the actin pixel intensity.

Figure 4

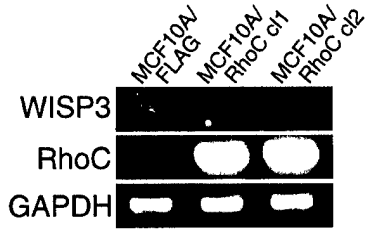

RhoC overexpression in MCF10A cells results in a decrease in WISP3 mRNA level. Reverse transcriptase polymerase chain reaction was conducted on vector and MCF10A cells stably overexpressing RhoC. RhoC-overexpressing cells had decreased levels of WISP3 mRNA.

by Western blotting. Restoration of WISP3 expression in SUM149 cells resulted in a decrease in RhoC protein expression in comparison with the empty vector control (Fig. 3). To investigate whether the relationship between WISP3 and RhoC expression is reciprocal, we developed MCF10A cells stably transfected with RhoC. These cells showed a 2.5-fold decrease in WISP3 mRNA expression (Fig. 4).

Discussion

Our previous work showed that the overexpression of RhoC GTPase and the loss of WISP3 expression are alterations that occur concordantly, more often in IBC than in slow-growing locally advanced breast cancers. WISP3 loss was found in concert with RhoC GTPase overexpression in 90% of archival patient samples of IBC, but rarely in stage-matched non-IBC tumors. Our laboratory further demonstrated that RhoC GTPase is a transforming oncogene for HME cells and that WISP3 has tumor inhibitory functions in IBC. However, neither alteration occurring in isolation seems to be sufficient to develop the full-blown, highly malignant IBC phenotype. Here we postulate that dysregulation of WISP3 might upregulate RhoC GTPase and thus enhance the aggressiveness of the phenotype that results when these two alterations are present.

We have shown that overexpression of RhoC GTPase in immortalized HME cells produced a striking tumorigenic effect that, for the most part, recapitulates the phenotype of the SUM149 IBC cell line. HME cells stably transfected with RhoC exhibited greatly increased growth under anchorage-independent conditions [15]. HME cells over-

expressing RhoC produced up to 100-fold more colonies than the controls, about 60% of the level of colony formation of the SUM149 IBC cell line. RhoC overexpression induced motility and invasion in HME cells, and markedly induced the production of angiogenic mediators including VEGF [17]. The HME/RhoC transfectants formed tumors when injected into the mammary fat pad of athymic nude mice [15].

Importantly, restoration of WISP3 in SUM149 cells ameliorated these features of the malignant phenotype. The SUM149/WISP3$^+$ cells exhibited decreased growth *in vitro* and *in vivo* in comparison with SUM149 cells transfected with the empty vector. The invasiveness of SUM149 cells was greatly decreased by restoring WISP3 expression. We also found that WISP3 markedly decreased the concentration of angiogenic mediators in the conditioned medium, especially VEGF, basic fibroblast growth factor, and interleukin-6 [9]. Given the high specificity of WISP3 and RhoC alterations in IBC and their interrelated functions in tumorigenesis, we propose that they cooperate in the development of IBC.

Using an antisense approach, inhibition of WISP3 expression in HME cells resulted in a threefold increase of RhoC GTPase transcript levels. The HME/AS WISP3 cells also exhibited increased cellular proliferation and anchorage-independent growth in soft agar. The HME/AS WISP3 cells produced significantly more colonies in soft agar in comparison with the control cells, an average of 58% of the level of colonies formed by the SUM149 IBC cells. HME/AS WISP3 cells also exhibited decreased production of VEGF in the conditioned medium.

The relationship between RhoC and WISP3 expression seems to be reciprocal. Restoration of WISP3 expression in SUM149 cells, which have lost WISP3 in the wild-type state, induced a 1.5-fold decrease in RhoC GTPase expression. These results are intriguing because changes in expression in Rho proteins by subtle factors such as 1.5–1.8 can be sufficient to modulate cellular behavior. Overexpression of RhoC in spontaneously immortalized HME cells, MCF10A, resulted in a 2.5-fold decrease in WISP3 mRNA expression.

In summary, overexpression of RhoC GTPase and loss of WISP3 are key genetic alterations in the development of IBC, and they have complementary functions. RhoC GTPase has a primary a role in motility, invasion, and angiogenesis [15,17]. WISP3 has a pivotal role in tumor growth, invasion, and angiogenesis [9]. Here we have further strengthened the evidence that these genes cooperate in the development of IBC, because WISP3 expression modulates the expression of RhoC GTPase and its functions.

Conclusion

IBC is the most lethal form of locally advanced breast cancer, with a 5-year disease-free survival of less than 45%. Our work focused on determining the genetic alterations that result in this aggressive breast cancer phenotype. Previously, we have found that RhoC and WISP3 are consistently and concordantly altered in IBC tissues. RhoC functions as an oncogene, and WISP3 as a tumor suppressor gene. Here we provide evidence supporting the hypothesis that these two genes act in concert to give rise to the highly aggressive IBC phenotype. We propose a model of this interaction as a starting point for further investigations.

Competing interests

None declared.

Acknowledgements

This work was supported in part by DOD grants DAMD17-02-1-0490 and DAMD17-02-1-0491 (CGK), DOD grants DAMD17-00-1-0345 and DAMD17-02-1-0492 (SDM), and NIH grants K08CA090876-01A2 (CGK), RO1CA77612 (SDM), P30CA46592 and M01-RR00042. We thank S Ethier for supplying the SUM149 and HME cell lines and R Kunkel for art work.

References

1. Jaiyesimi IA, Buzdar AU, Hortobagyi G: **Inflammatory breast cancer: a review.** *J Clin Oncol* 1992, **10**:1014-1024.
2. Lee BJ, Tannenbaum ND: **Inflammatory carcinoma of the breast: a report of twenty-eight cases from the breast clinic of Memorial Hospital.** *Surg Gynecol Obstet* 1924, **39**:580-595.
3. Merajver SD, Weber BL, Cody R, Zhang D, Strawderman M, Calzone KA, LeClaire V, Levin A, Irani J, Halvie M, August D, Wicha M, Lichter A, Pierce LJ: **Breast conservation and prolonged chemotherapy for locally advanced breast cancer: the University of Michigan experience.** *J Clin Oncol* 1997, **15:** 2873-2881.
4. Swain SM, Sorace RA, Bagley CS, Danforth DN Jr, Bader J, Wesley MN, Steinberg SM, Lippman ME: **Neoadjuvant chemotherapy in the combined modality approach of locally advanced nonmetastatic breast cancer.** *Cancer Res* 1987, **47:** 3889-3894.
5. van Golen KL, Davies S, Wu ZF, Wang Y, Bucana CD, Root H, Chandrasekharappa S, Strawderman M, Ethier SP, Merajver SD: **A novel putative low-affinity insulin-like growth factor-binding protein, LIBC (lost in inflammatory breast cancer), and RhoC GTPase correlate with the inflammatory breast cancer phenotype.** *Clin Cancer Res* 1999, **5**:2511-2519.
6. Perbal B: **NOV (nephroblastoma overexpressed) and the CCN family of genes: structural and functional issues.** *Mol Pathol* 2001, **54**:57-79.
7. Pennica D, Swanson TA, Welsh JW, Roy MA, Lawrence DA, Lee J, Brush J, Taneyhill LA, Deuel B, Lew M, Watanabe C, Cohen RL, Melhem MF, Finley GG, Quirke P, Goddard AD, Hillan KJ, Gurney AL, Botstein D, Levine AJ: **WISP genes are members of the connective tissue growth factor family that are up-regulated in wnt-1-transformed cells and aberrantly expressed in human colon tumors.** *Proc Natl Acad Sci USA* 1998, **95**:14717-14722.
8. Hurvitz JR, Suwairi WM, Van Hul W, El-Shanti H, Superti-Furga A, Roudier J, Holderbaum D, Pauli RM, Herd JK, Van Hul EV, Rezai-Delui H, Legius E, Le Merrer M, Al-Alami J, Bahabri SA, Warman ML: **Mutations in the CCN gene family member WISP3 cause progressive pseudorheumatoid dysplasia.** *Nat Genet* 1999, **23**:94-98.
9. Kleer CG, Zhang Y, Pan Q, van Golen KL, Wu ZF, Livant D, Merajver SD: **WISP3 is a novel tumor suppressor gene of inflammatory breast cancer.** *Oncogene* 2002, **21**:3172-3180.
10. Kimura K, Ito M, Amano M, Chihara K, Fukata Y, Nakafuku M, Yamamori B, Feng J, Nakano T, Okawa K, Iwamatsu A, Kaibuchi

K: **Regulation of myosin phosphatase by Rho and Rho-associated kinase (Rho-kinase).** *Science* 1996, **273**:245-248.
11. Leung T, Chen XQ, Manser E, Lim L: **The p160 RhoA-binding kinase ROK alpha is a member of a kinase family and is involved in the reorganization of the cytoskeleton.** *Mol Cell Biol* 1996, **16**:5313-5327.
12. Nobes CD, Hall A: **Rho, rac, and cdc42 GTPases regulate the assembly of multimolecular focal complexes associated with actin stress fibers, lamellipodia, and filopodia.** *Cell* 1995, **81**: 53-62.
13. Ethier SP, Mahacek ML, Gullick WJ, Frank TS, Weber BL: **Differential isolation of normal luminal mammary epithelial cells and breast cancer cells from primary and metastatic sites using selective media.** *Cancer Res* 1993, **53**:627-635.
14. Band V, Zajchowski D, Kulesa V, Sager R: **Human papilloma virus DNAs immortalize normal human mammary epithelial cells and reduce their growth factor requirements.** *Proc Natl Acad Sci USA* 1990, **87**:463-467.
15. van Golen KL, Wu ZF, Qiao XT, Bao LW, Merajver SD: **RhoC GTPase, a novel transforming oncogene for human mammary epithelial cells that partially recapitulates the inflammatory breast cancer phenotype.** *Cancer Res* 2000, **60**:5832-5838.
16. Kleer CG, van Golen KL, Zhang Y, Wu ZF, Rubin MA, Merajver SD: **Characterization of RhoC expression in benign and malignant breast disease : a potential new marker for small breast carcinomas with metastatic ability.** *Am J Pathol* 2002, **160**:579-584.
17. van Golen KL, Wu ZF, Qiao XT, Bao L, Merajver SD: **RhoC GTPase overexpression modulates induction of angiogenic factors in breast cells.** *Neoplasia* 2000, **2**:418-425.

Correspondence

Sofia D Merajver, 7217 CCGC, 1500 East Medical Center Drive, Ann Arbor, MI 48109-0948, USA. Tel: +1 734 936 6884; fax: +1 734 936 7376; e-mail: smerajve@umich.edu

RESEARCH ARTICLE

Neoplasia • Vol. 6, No. 2, March/April 2004, pp. 179–185 179

www.neoplasia.com

WISP3 (CCN6) Is a Secreted Tumor-Suppressor Protein that Modulates IGF Signaling in Inflammatory Breast Cancer[1]

Celina G. Kleer, Yanhong Zhang*, Quintin Pan† and Sofia D. Merajver†*

Departments of *Pathology and †Internal Medicine, Division of Hematology and Oncology, University of Michigan Medical Center, Ann Arbor, MI, USA

Abstract

Inflammatory breast cancer (IBC) is the most lethal form of locally advanced breast cancer. We have found that WISP3 is lost in 80% of human IBC tumors and that it has growth- and angiogenesis-inhibitory functions in breast cancer *in vitro* and *in vivo*. WISP3 is a cysteine-rich, putatively secreted protein that belongs to the CCN family. It contains a signal peptide at the N-terminus and four highly conserved motifs. Here, for the first time, we investigate the function of WISP3 protein in relationship to its structural features. We found that WISP3 is secreted into the conditioned media and into the lumens of normal breast ducts. Once secreted, WISP3 was able to decrease, directly or through induction of other molecule(s), the IGF-1–induced activation of the IGF-IR, and two of its main downstream signaling molecules, IRS1 and ERK-1/2, in SUM149 IBC cells. Furthermore, WISP3 containing conditioned media decreased the growth rate of SUM149 cells. This work sheds light into the mechanism of WISP3 function by demonstrating that it is secreted and that, once in the extracellular media, it induces a series of molecular events that leads to modulation of IGF-IR signaling pathways and cellular growth in IBC cells.

Neoplasia (2004) **6**, 179–185

Keywords: IGF-binding proteins, MAPK signaling, cell proliferation, cell cycle control, ERK-1/2 phosphorylation.

Introduction

Inflammatory breast cancer (IBC) is the most lethal form of locally advanced breast cancer [1,2]. It is also a very distinct clinical and pathological type of carcinoma. Clinically, patients present with what has been classically termed "peau d'orange," characterized by skin thickening and dimpling, also with nodularity, erythema, and, often, nipple retraction [1–4]. IBC is highly angiogenic and angioinvasive. Clusters of malignant cells invade the dermal lymphatics, forming tumor emboli that likely cause the clinical symptoms, and disseminate to distant sites [1].

In our previous work, we found that WISP3 is lost in 80% of human IBC tumors and is a key genetic determinant of the IBC phenotype [5]. WISP3 has growth-, invasion-, and angiogenesis-inhibitory functions in IBC *in vitro* and *in vivo* [6]. WISP3 is a member of the CCN family of proteins, which also includes connective tissue growth factor (CTGF), Cyr61, Nov, WISP1, and WISP2 [7,8]. A putatively secreted protein with a secretory signal peptide at the NH_2 terminus, WISP3 contains 36 conserved cysteine residues that are organized into four highly conserved modules: 1) a motif associated with insulin-like growth factor binding protein (IGFBP) (GCGCCXXC); 2) a von Willebrand type C–like motif; 3) a thrombospondin 1 module; and 4) a carboxyl-terminal domain putatively involved in dimerization [8,9]. The role of each of these conserved domains in the function of the CCN proteins, in general, and of WISP3, in particular, remains to be elucidated.

IGF-I and its major receptor, IGF-IR, play an important role in normal breast biology and in the development of breast cancer [10–13]. A large body of work implicates the IGF family in breast cancer progression. High concentrations of IGF-I in serum are associated with increased mammographic density (one of the strongest predictors of breast cancer risk), and also reliably predict increased breast cancer risk specifically in premenopausal women [14]. *In vitro*, IGF-I is a strong mitogen for human breast cancer cells and has been found in the epithelial and stromal component of breast cancers [13]. High expression of IGF-IR has been demonstrated in most primary human breast cancers when compared to normal or benign breast tissues, and hyperactivation of IGF-IR in breast cancer has been linked to increased radioresistance and cancer recurrence at the primary site [13,15,16]. High levels of IRS-1, a major signaling molecule downstream of the IGF-IR, correlate with tumor size and shorter disease-free survival in ER^+ breast cancer patients [17,18]. Based on the protein sequence of WISP3 and the important role of IGF signaling in breast cancer, we hypothesized that WISP3 is secreted into the extracellular medium and that the growth-inhibitory effect of

Address all correspondence to: Sofia D. Merajver, MD, PhD, and Celina G. Kleer, MD, Department of Internal Medicine, 7217 CCGC, 1500 East Medical Center Drive, Ann Arbor, MI 48108-0948, USA. E-mail: smerajve@umich.edu

[1]This work was supported, in part, by Army grants DAMD17-02-1-0490 (C.G.K.), DAMD17-02-1-491 (C.G.K.), and DAMD-17-00-1-0345 (S.D.M.); National Institutes of Health grants K08CAO9O876 (C.G.K.), RO1CA77612 (S.D.M.) and 1 P50-CADE97258 (S.D.M.); and a grant from the John and Suzanne Munn Endowed Research Fund of the University of Michigan Comprehensive Cancer Center (C.G.K.).

Received 5 September 2003; Revised 2 December 2003; Accepted 3 December 2003.

DOI 10.1593/neo.03316

WISP3 in IBC may be dependent, at least in part, on modulation of IGF-I signaling. To test this hypothesis, we investigated the downstream effects of WISP3 starting at the IGF-IR receptor and signaling pathway. Here, we demonstrate that WISP3 is a secreted protein and that, once in the conditioned media, it can effectively modulate IGF-IR activation and its signaling cascade and the cellular growth of IBC cells.

Materials and Methods

Cell Culture and Transfections

SUM149 cells derive from a primary IBC that has lost WISP3 expression [6,19]. SUM149 cells and their transfectants were cultured in Ham's F-12 media supplemented with 5% fetal bovine serum (FBS), hydrocortisone (1 μg/ml), insulin (5 μg/ml), fungizone (2.5 μg/ml), gentamycin (5 μg/ml), and penicillin/streptomycin (100 μ/ml each), at 37°C under 10% CO_2. HEK-293 cells derived from human embryonic kidney epithelial cells were grown in Dulbecco's modified Eagle's medium (DMEM) containing 10% FBS. SUM149 and HEK-293 cells were transfected with HIS^- tagged (pcDNA 3.1/V5-HIS TOPO TA expression vector; Invitrogen, Carlsbad, CA) and $Flag^-$ tagged (pFlag-CMV vector; Sigma, St. Louis, MO) full-length WISP3 cDNA, and clonal cell lines were established as described previously [6]. Control cell lines were generated by transfecting the SUM149 and HEK-293 cell lines with the empty vectors. The inserts were confirmed by sequencing. Cells were incubated in serum-free medium. WISP3 and control conditioned media were collected 3 days later. The conditioned media were cleared of cell debris by centrifugation, and concentrated 10-fold through a Centriplus YM-10 column (Millipore, Bedford, MA) before use.

IGF-I Stimulation

Seventy percent confluent SUM149 cells were shifted to serum-free medium. After 24 hours of starvation, the cells were cultured in WISP3 and control conditioned media for 24 hours. Subsequently, SUM149 cells were stimulated with 20 ng/ml human recombinant IGF-I (Upstate Biotechnology Inc., Lake Placid, NY) for 15 minutes.

Immunoprecipitation and Western Blotting

Cells were lysed in lysis buffer composed of 50 mM Tris–HCl (pH 7.4), 150 mM NaCl, 1% NP-40, 0.25% sodium deoxycholate, 1 mM EGTA, 1 mM Na_3VO_4, 1 mM PMSF, and 1 μg/ml aprotinin. The lysates were clarified by centrifugation at 14,000*g* for 10 minutes. A total of 500 μg of cell lysates was incubated with 1 μg/ml anti–IGF-IR mAb (Calbiochem, San Diego, CA) overnight at 4°C. Immune complexes were precipitated by adding 50 μl of protein A/G plus agarose bead slurry for 2 hours. The agarose beads were collected and washed three times with ice-cold lysis buffer, and resuspended in 25 μl of 2 × Laemmli sample buffer for sodium dodecyl sulfate polyacrylamide gel electrophoresis (SDS-PAGE). Fifty micrograms of protein extract was separated by SDS-PAGE and transferred onto a PVDF membrane (Amersham Pharmacia Biotech). The precipitated IGF-IR was detected with anti–IGF-IR β subunit polyclonal Ab (Santa Cruz Biotechnology, Santa Cruz, CA). Tyrosine phosphorylation of immunoprecipitated IGF-IR was assessed with anti–phosphotyrosine mAB PY20 (Transduction Laboratories, Lexington, KY). Total IGF-IR, phosphorylated and total IRS1, and ERK-1/2 were measured with appropriate antibodies (Transduction Laboratories; Upstate Biotechnology Inc.). WISP3 expression was confirmed by Western blot using a polyclonal anti–WISP3 antibody (gift from Dr. Warman) and an antibody against the HIS tag (Invitrogen). The protein bands were visualized using enhanced chemiluminescence (Amersham Pharmacia Biotech, Piscataway, NJ). All experiments were repeated at least three times and the optical density of the bands was quantified by densitometry (Scio Image software for Win 95/98, version 0.4). Statistical analysis was performed using 95% confidence intervals for the estimates of the means. A P value of $< .05$ was considered statistically significant.

Effect of WISP3 in the Proliferation of SUM149 cells

SUM149 cells were plated in 96-well tissue culture plates at a density of 5×10^4 cells/ml in Ham's F-12 media with 5% FBS. One hundred microliters of serum-free medium was added for 24 hours. Ten-fold concentrated WISP3 and control conditioned media were added in the presence and absence of IGF-I simulation as described above. MTT reagents were added 24 hours later according to the manufacturer's protocol (Sigma), and the plate was read at a wavelength of 595 nm. The experiment was performed in triplicate.

Human Breast Tissues and Immunohistochemistry

WISP3 protein expression was studied by immunohistochemistry in normal human breast tissues obtained from 10 reduction mammoplasty procedures. Immunohistochemical analysis was performed by using a polyclonal anti–WISP3 antibody at 1:500 dilution with overnight incubation and microwave antigen retrieval [20]. The detection reaction followed the Dako Envision$^+$ System Peroxidase kit protocol (Dako, Carpinteria, CA). Diaminobenzidine was used as chromogen and hematoxylin was used as counterstain. Positive and negative controls were tumor xenografts derived from cell lines shown to express high levels of WISP3 (SUM149 cell line stably transfected with WISP3) and from a cell line that does not express WISP3 (SUM149 wild type), respectively.

Results

WISP3 Protein Is Secreted by Human Breast Epithelial Cells

WISP3 protein contains a multimodular structure with a secretory signal peptide at the N-terminus. To investigate whether WISP3 is secreted by breast epithelial cells, SUM149 IBC cells previously characterized with a loss in WISP3 expression were stably transfected to express full-length WISP3. Conditioned media from SUM149/WISP3–overexpressing clones were collected and

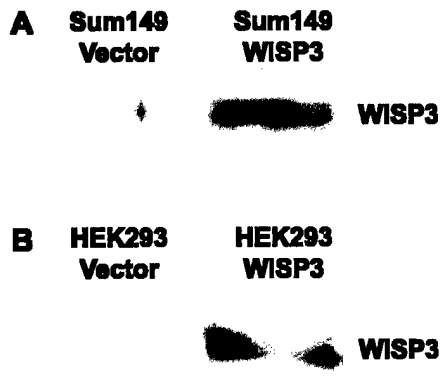

Figure 1. *WISP3 protein is secreted and detected in the conditioned media. (A) Western immunoblot using anti–WISP3 polyclonal antibody detects WISP3 protein in the conditioned media of SUM149 cells transfected with WISP3 full-length cDNA. WISP3 protein is not detected in the conditioned media of SUM149 cells transfected with the empty vector. (B) Western immunoblot of the conditioned media of HEK-293 cells transfected with WISP3, detected using an anti–HIS antibody. WISP3 is not detected in the conditioned media of the control cells.*

detected for WISP3 by Western blot analysis using a polyclonal anti–WISP3 antibody. WISP3 protein was detected in the media of SUM149-expressing WISP3 (SUM149/WISP3), and not in the media of empty vector–transfected SUM149 cells (SUM149/Flag) (Figure 1*A*). In order to explore these results from a different perspective, we performed transient transfections of WISP3 in SUM149 cells using a HIS^- tagged full-length WISP3 expression vector. In this case, WISP3 protein was detected in the conditioned media using both anti–WISP3 antibody and anti–HIS antibody (data not shown). To specifically address whether WISP3 would be detected in the conditioned media of a nonmammary cell, we repeated these experiments with the HEK293 cell line, derived from human embryonic kidney epithelial cells. WISP3 was detected in the conditioned media of these cells and not in the conditioned media of the empty vector controls (Figure 1*B*).

In situ expression of WISP3 protein was determined by immunohistochemical analysis of normal breast tissues derived from reduction mammoplasty procedures. In all 10 tissues examined, WISP3 protein was expressed at low levels in the cytoplasm of normal epithelial cells from ducts and acini and, interestingly, was present in the luminal secretions of ducts and lobules (Figure 2*A*). Xenografts derived from wild-type SUM149 cells ($WISP3^-$) and from SUM149/$WISP3^+$ cells were used as negative and positive controls, respectively (Figure 2, *B* and *C*).

WISP3 Containing Conditioned Media Reduces IGF-I–Induced IGF-IR Activation and Signaling Pathways

The effect of WISP3 on the activation of the IGF-I signaling pathway was studied in SUM149 cells derived from a primary IBC [5,6,19,21]. The activation of the IGF signaling

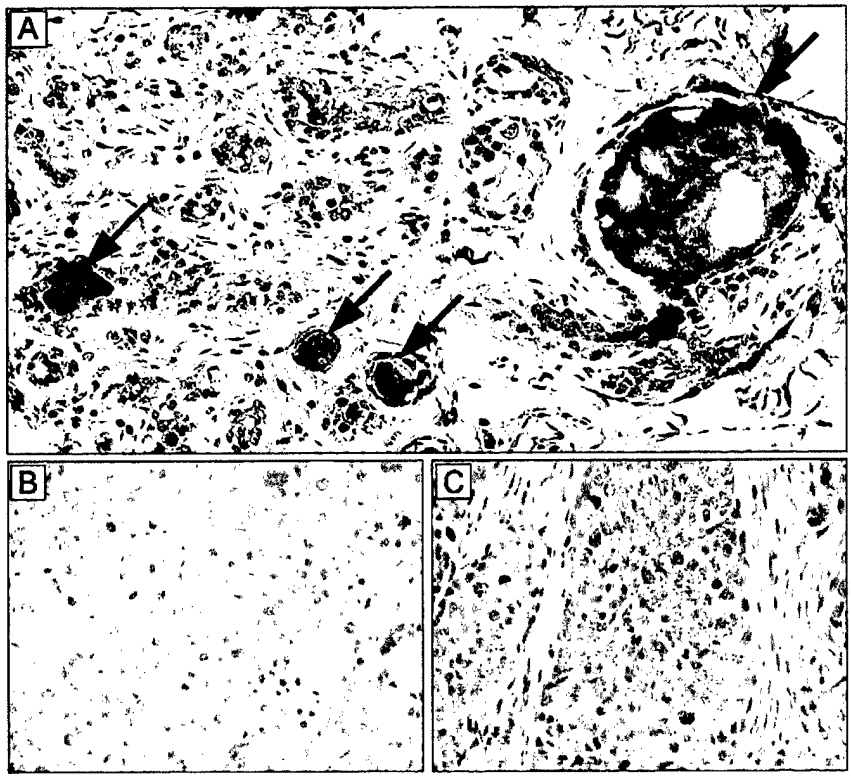

Figure 2. *In situ expression of WISP3 protein in normal breast tissues. (A) Immunohistochemical analysis of normal breast tissues using a polyclonal anti–WISP3 antibody shows that WISP3 protein is expressed at low levels in the cytoplasm of normal epithelial cells and in the luminal secretions of ducts and acini (arrows) (× 200). (B and C) Xenografts derived from wild-type SUM149 and SUM149/WISP3 cells were used as negative and positive controls, respectively (× 400).*

cascade plays a central role in breast cancer development and progression. To investigate whether the presence of WISP3 in the conditioned media has an effect on IGF-IR signaling pathways in IBC cells, phosphorylation of IGF-IR, IRS1, and ERK-1/2 was determined in wild-type SUM149 cells in the presence or absence of WISP3 in the conditioned media. Experiments were carried out under baseline conditions without addition of IGF-I and after stimulation with IGF-I. In the presence of WISP3 in the conditioned media, SUM149 cells exhibited decreased IGF-IR phosphorylation (Figure 3). The effect of WISP3 in the phosphorylation of the IGF-IR was evident in the presence of IGF-I stimulation because WISP3 was able to ameliorate the effect of IGF-I stimulation on the activation of the IGF-IR (Figure 3). Similarly, WISP3 conditioned media decreased the IGF-I–induced IRS1 and ERK-1/2 phosphorylation (Figures 4 and 5).

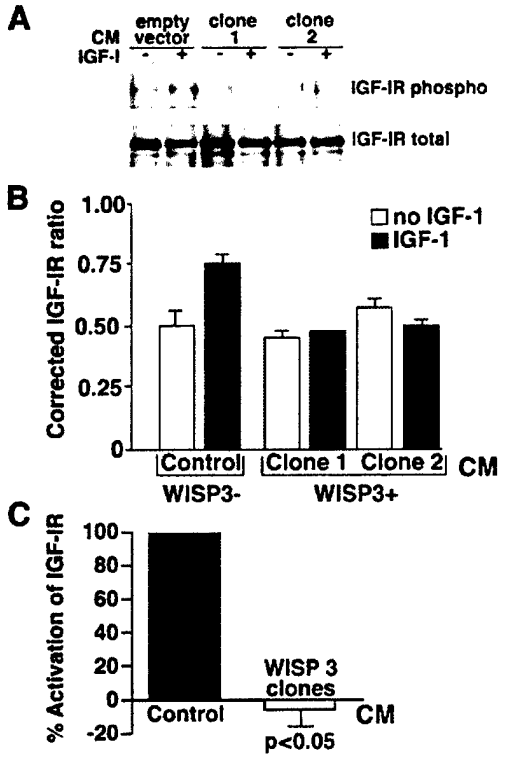

Figure 3. *WISP3 decreases IGF-I–induced phosphorylation of the IGF-IR. (A) Western blot analysis of SUM149 cell lines bathed in WISP3$^+$ and control (WISP3$^-$) conditioned media. The experiment was carried out under baseline conditions (without IGF-I) and after stimulation with 20 ng/ml IGF-I. The IGF-IR was precipitated from 500 μg of protein lysate with an anti–IGF-IR mAb and subsequently detected by immunoblot with an anti–IGF-IR β subunit polyclonal Ab. Tyrosine phosphorylation of immunoprecipitated IGF-IR was assessed with an anti–phosphotyrosine mAb PY20. (B) Relative protein levels of IGF-IR phosphorylation normalized for total IGF-IR. Blots were scanned and the pixel intensity measured using Scn Image program. Results are expressed as mean ± SEM of three independent experiments. (C) Quantitation of the differences in the percent activation of the IGF-IR. The difference in normalized IGF-IR phosphorylation under baseline conditions and after IGF-I stimulation was calculated for each cell line. Results were corrected using the difference in IGF-IR phosphorylation in the absence of IGF-I stimulation as reference. WISP3 was able to decrease the IGF-I–induced activation of the IGF-IR (t test, P < .05).*

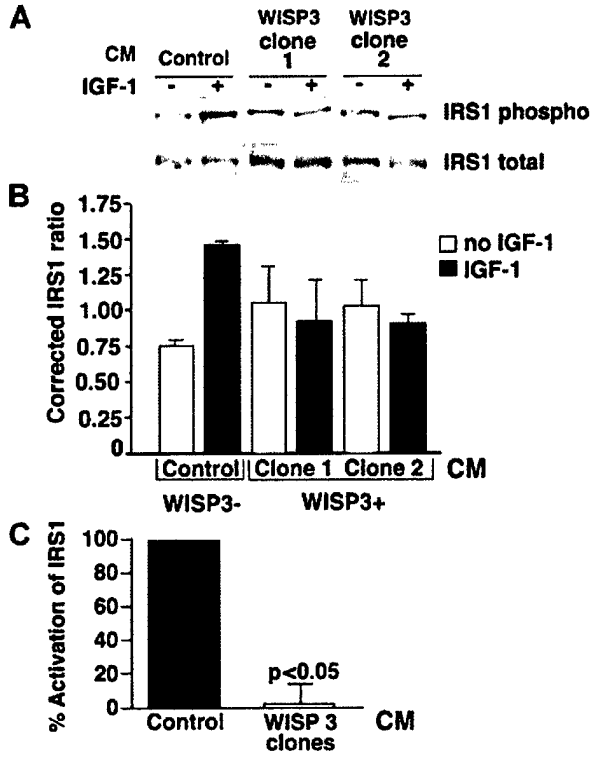

Figure 4. *WISP3 decreases IGF-I–induced phosphorylation of IRS1. (A) Western blot analysis of SUM149 cell lines bathed in WISP3$^+$ and control WISP3-conditioned media. The experiment was carried out under baseline conditions (without IGF-I) and after stimulation with IGF-I. The expression of phosphorylated IRS1 was detected by Western blot using a polyclonal antibody against phosphorylated IRS1. The Western blot was stripped and probed with an antibody against total IRS1. (B) Relative protein levels of IRS1 phosphorylation normalized for total IRS1. Blots were scanned and the pixel intensity measured. Results are expressed as mean ± SEM of three independent experiments. (C) The differences in the percent activation of IRS-1 were quantitated. The difference in the corrected IRS1 phosphorylation under baseline conditions and after IGF-I stimulation was calculated for each cell line and results were normalized using the difference in IRS1 phosphorylation in the absence of IGF-I stimulation as reference. WISP3-rich conditioned media was able to decrease the phosphorylation of IRS-1 triggered by IGF-I (t test, P < .05).*

WISP3 Containing Conditioned Media Reduces the Growth of IBC Cell Lines

After establishing that the presence of WISP3 in the conditioned media was able to modulate IGF-I signaling pathways, its effect on cellular proliferation was determined in the presence and absence of IGF-I stimulation. SUM149 cells bathed in the WISP3 conditioned media had significantly lower growth rates than the control SUM149 cells bathed in control (WISP3-deficient) conditioned media, both in the presence and absence of IGF-I stimulation (*t* test, $P < .05$; Figure 6).

Discussion

We have previously demonstrated that WISP3 is lost in 80% of IBC tumors and that it has tumor-suppressor functions in IBC [5,6]. Studies on the SUM149 IBC cell line showed that restoration of WISP3 expression has potent growth- and

angiogenesis-inhibitory functions *in vitro* and *in vivo* [6]. Restoration of WISP3 resulted in a significant decrease in anchorage-independent growth in soft agar and cellular proliferation, as well as a drastic decrease in the invasive capabilities of the SUM149 cells, which are highly invasive in their wild-type state. Furthermore, restoration of WISP3 expression in SUM149 cells resulted in a biologically relevant decrease in the level of angiogenic factors (VEGF, bFGF, and IL-6) in the conditioned media of the cells. *In vivo*, restoration of WISP3 expression in SUM149 cells caused a drastic decrease in tumor volume and rate of tumor growth when injected in nude mice [6]. Taken together, this body of work had strongly supported a tumor-suppressor role for WISP3 in mammary tumor progression. In the present study, we sought to discover the molecular mechanisms underlying the tumor-suppressor function of WISP3.

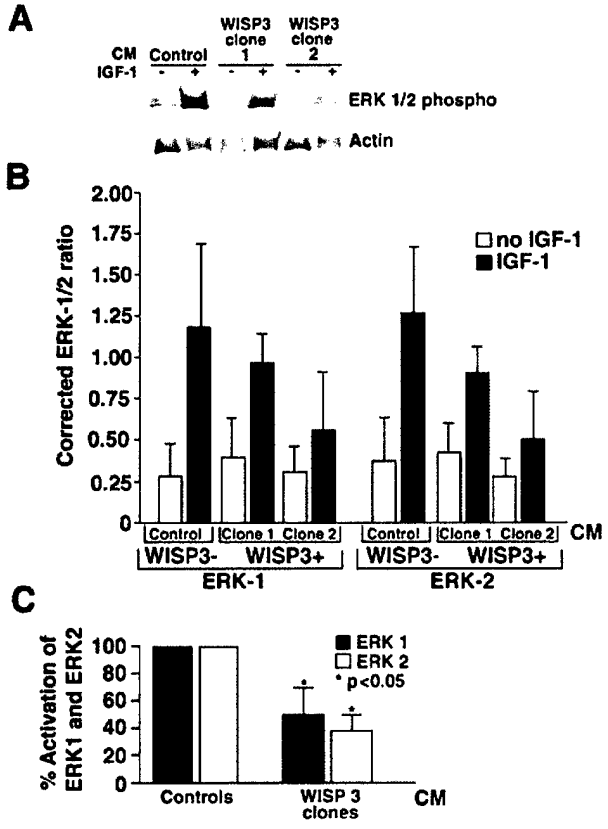

Figure 5. *WISP3 decreases IGF-I–induced phosphorylation of ERK-1/2. (A) Western blot analysis of SUM149 cell lines bathed in WISP3⁺ and control (WISP3⁻) conditioned media, under baseline conditions (without IGF-I) and after stimulation with IGF-I. The expression of ERK-1/2 was detected by Western blot using a polyclonal antibody against phosphorylated ERK-1/2. The blot was stripped and probed with an antibody against β-actin. (B) Relative protein levels of ERK-1/2 phosphorylation normalized using actin. Blots were scanned and the pixel intensity measured. Results are expressed as mean ± SEM of three independent experiments. (C) Quantitation of the differences in the percent activation of ERK-1/2. The difference in the corrected ERK-1/2 phosphorylation under baseline conditions and after IGF-I stimulation was calculated for each cell line. Results were normalized using the difference in ERK-1/2 phosphorylation in the absence of IGF-I stimulation as reference. WISP3-rich conditioned media ameliorated the phosphorylation of ERK 1 and ERK 2 induced by IGF-I stimulation (t test, P < .05).*

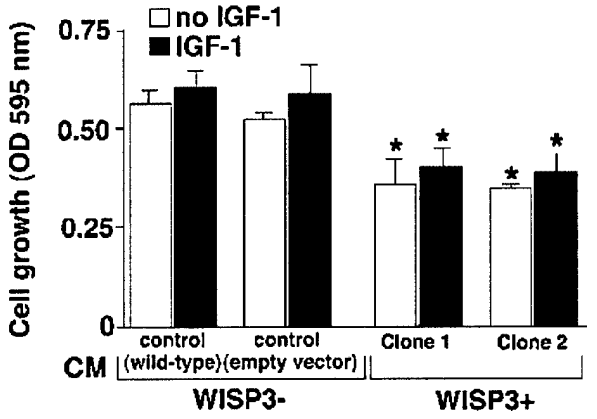

Figure 6. *WISP3 decreases the growth of IBC cells. The growth of SUM149 cells was measured in the absence (WISP3⁻) and presence of WISP3 (WISP3⁺) in the conditioned media under baseline conditions (no IGF-I) and after IGF-I stimulation by an MTT assay. SUM149 cells were grown in 96-well plates at a density of 5 × 10⁴ cells/ml. Serum-starved cells were incubated for 24 hours in the WISP3 and control conditioned media, with or without IGF-I stimulation. Results are expressed as mean ± SEM of three independent experiments. WISP3⁺ conditioned media decreases significantly the growth of SUM149 cells (t test, P < .05 for both clones).*

WISP3 belongs to the CCN family of proteins, which are highly conserved, putatively secreted proteins with important roles in development during chondrogenesis and skeletogenesis [7]. The CCN proteins have been recently also implicated in carcinogenesis [7,22–26]. It is not well understood, however, how the functions of the CCN proteins in development relate to their role in cancer. Moreover, their expression during tumorigenesis cannot be generalized across different tissue types. This may be due to tissue-specific functions of the CCN proteins, perhaps mediated by their multimodular structure and the presence of different affinities for binding partners and ligands in different tissues [7]. The presence of different receptors and differential processing of the CCN proteins (e.g., cleavage by proteases) may account also for their diverse functions in different tissues. In this paper, we focused on determining whether WISP3 is secreted into the conditioned media and its relationship to IGF signaling pathways.

Analysis of the protein sequence of WISP3 revealed that it contains a signal peptide at the N-terminal region that may participate in the secretion of the protein into the extracellular media [7–9]. Indeed, by Western blot, using two different specific antibodies, we were able to detect WISP3 protein in the conditioned media of SUM149 and HEK293 cells transfected with WISP3. Furthermore, consistent with these results, by immunohistochemical analysis, WISP3 protein was detected in the secretions accumulated in the lumens of ducts and lobules in normal breast tissues. The fact that WISP3 is secreted and present in the conditioned media (thereby alluding to its stability in solution) led us to the hypothesis that it may directly or indirectly regulate IGF signaling.

Although the signaling pathways that are required for the effects of IGF-I in breast cancer have not been completely elucidated, the contribution of IGF-I–induced IGF-IR

activation appears to be critical in hormone-dependent and -independent breast cancer [27–30]. IGF-I is locally released by breast cancer cells and stromal fibroblasts, and it is involved in autocrine and paracrine stimulation of the mammary epithelium [31]. In breast cancer cells, when IGF-I binds IGF-IR, signaling occurs mainly through activation of IRS-1 and RAS-dependent phosphorylation of MAP kinase with subsequent activation of nuclear transcription factors [32,33]. IGF-I signaling promotes cell growth, survival, and motility of breast cancer cells, as well as resistance to therapeutic interventions [10–12,14–18]. We hypothesized that expression of WISP3 could result in a series of molecular events that leads to the modulation of IGF-IR activation and downstream signaling. Contributing to this hypothesis is the fact that we have shown that WISP3 is secreted into the media where it has the opportunity to directly or indirectly modulate the strength of IGF signaling. Indeed, in the presence of IGF-I, WISP3 containing conditioned media decreased IGF-IR phosphorylation and the phosphorylation of two main downstream IGF-IR signaling molecules, IRS1 and ERK-1/2. This inhibition was not evident under baseline conditions, without stimulation with IGF-I. Our experiments thus show that even relatively small concentrations of WISP3 secreted by WISP3-transfected cells are able to modulate, directly or indirectly, IGF-I signaling in the setting of IGF-I stimulation.

A major growth-regulatory IGF-IR downstream pathway that regulates breast cancer growth and survival converges on ERK-1/2 cascade [34]. We observed a decrease in ERK-1/2 phosphorylation by addition of WISP3 containing conditioned media in the presence of IGF-I stimulation. ERK-1/2 influence chromatin remodeling and activation of gene expression, leading to enhanced cellular proliferation and decreased apoptosis [35–37]. Specifically, ERK-1/2 have been shown to activate the transcription of key genes involved in cell cycle progression including cyclin D1 and cyclin E. We have shown previously that restoration of WISP3 expression in the highly malignant SUM149 IBC cell line markedly decreased the levels of cyclin E and PCNA, a reliable marker of cellular proliferation [6].

The mechanism whereby WISP3 may modulate IGF-IR activation in the presence of IGF-I remains to be elucidated. WISP3 contains a highly conserved motif (GCGCCXXC) characteristic of IGFBPs, which may provide the proper protein folding to interact with IGF-like ligands, thereby enabling interference with IGF signaling. Although initial studies reported that two other CCN proteins, CTGF (CTGF) and Nov, specifically bind to IGF-I [38,39], these results have not been subsequently built on and they remain to be duplicated by other investigators. Whether WISP3 physically binds to IGF-I warrants further investigation, in light of out data.

Another mechanism that may explain the modulation of IGF-IR phosphorylation by WISP3-containing conditioned media is the formation of a WISP3/IGF-I complex that may bind to the IGF-IR and occupy IGF binding sites, but the complex may be either inhibitory or may be only a weak agonist of the receptor. In another system [40], this hypothesis is supported by recent data showing that IGF-I can still freely bind to the receptor even when complexed to a truncated N-terminal fragment of IGF-binding protein 5 (mini-IGFBP5); interestingly, the N-terminal portion of IGFBP5 has high homology to the N-terminal portion of WISP3. Mini-IGFBP5 binding to IGF-I resulted in incomplete inhibition of receptor binding [40]. In a similar manner, a WISP3/IGF-I complex might still bind to the IGF-IR but exert only a weak agonist effect, effectively resulting in physiologic antagonism of IGF-I action under conditions of high IGF-I stimulation. WISP3-rich conditioned media was able to significantly decrease the proliferation rate of IBC cells. The fact that this effect was seen both in the presence and absence of IGF-I simulation suggests that, in addition to interfering with IGF-I signaling pathways, WISP3 may have IGF-independent functions in IBC. In sum, we show that WISP3 is a secreted protein that modulates IGF-I signaling pathways, leading to a decrease in the growth of IBC cells.

Acknowledgements

We thank Robin Kunkel and Elizabeth Horn for artwork; S. Ethier for the SUM149 and HME cell lines; Wendy Kutz and Matthew Warman from Case Western Reserve University for providing anti–WISP3 antibody; and Michelle LeBlanc and the Immunohistochemistry Core of the University of Michigan Cancer Center for tissue processing and immunohistochemistry.

References

[1] Lee BJ (1924). Inflammatory carcinoma of the breast: a report of twenty-eight cases from the breast clinic of Memorial Hospital. *Surg Gynecol Obstet* **39,** 580–595.

[2] Jaiyesimi IA, Buzdar AU, and Hortobagyi G (1992). Inflammatory breast cancer: a review. *J Clin Oncol* **10,** 1014–1024.

[3] Merajver SD, Weber BL, Cody R, Zhang D, Strawderman M, Calzone KA, LeClaire V, Levin A, Irani J, Helvie M, August D, Wicha M, Lichter A, and Pierce LJ (1997). Breast conservation and prolonged chemotherapy for locally advanced breast cancer: the University of Michigan experience. *J Clin Oncol* **15,** 2873–2881.

[4] Swain SM, Sorace RA, Bagley CS, Danforth Jr, DN, Bader J, Wesley MN, Steinberg SM, and Lippman ME (1987). Neoadjuvant chemotherapy in the combined modality approach of locally advanced nonmetastatic breast cancer. *Cancer Res* **47,** 3889–3894.

[5] van Golen KL, Davies S, Wu ZF, Wang Y, Bucana CD, Root H, Chandrasekharappa S, Strawderman M, Ethier SP, and Merajver SD (1999). A novel putative low-affinity insulin-like growth factor–binding protein, LIBC (lost in inflammatory breast cancer), and RhoC GTPase correlate with the inflammatory breast cancer phenotype. *Clin Cancer Res* **5,** 2511–2519.

[6] Kleer CG, Zhang Y, Pan Q, van Golen KL, Wu ZF, Livant D, and Merajver SD (2002). *WISP3* is a novel tumor suppressor gene of inflammatory breast cancer. *Oncogene* **21,** 3172–3180.

[7] Perbal B (2001). *NOV* (nephroblastoma overexpressed) and the *CCN* family of genes: structural and functional issues. *Mol Pathol* **54,** 57–79.

[8] Pennica D, Swanson TA, Welsh JW, Roy MA, Lawrence DA, Lee J, Brush J, Taneyhill LA, Deuel B, Lew M, Watanabe C, Cohen RL, Melhem MF, Finley GG, Quirke P, Goddard AD, Hillan KJ, Gurney AL, Botstein D, and Levine AJ (1998). *WISP* genes are members of the connective tissue growth factor family that are up-regulated in wnt-1–transformed cells and aberrantly expressed in human colon tumors. *Proc Natl Acad Sci USA* **95,** 14717–14722.

[9] Hurvitz JR, Suwairi WM, Van Hul W, El-Shanti H, Superti-Furga A, Roudier J, Holderbaum D, Pauli RM, Herd JK, Van Hul EV, Rezai-Delui

H, Legius E, Le Merrer M, Al-Alami J, Bahabri SA, and Warman ML (1999). Mutations in the *CCN* gene family member *WISP3* cause progressive pseudorheumatoid dysplasia. *Nat Genet* **23,** 94–98.

[10] Bartucci M, Morelli C, Mauro L, Ando S, and Surmacz E (2001). Differential insulin-like growth factor I receptor signaling and function in estrogen receptor (ER)–positive MCF-7 and ER-negative MDA-MB-231 breast cancer cells. *Cancer Res* **61,** 6747–6754.

[11] Furstenberger G, and Senn HJ (2002). Insulin-like growth factors and cancer. *Lancet Oncol* **3,** 298–302.

[12] Kleinberg DL, Feldman M, and Ruan W (2000). IGF-I: an essential factor in terminal end bud formation and ductal morphogenesis. *J Mammary Gland Biol Neoplasia* **5,** 7–17.

[13] Surmacz E (2000). Function of the IGF-I receptor in breast cancer. *J Mammary Gland Biol Neoplasia* **5,** 95–105.

[14] Byrne C, Colditz GA, Willett WC, Speizer FE, Pollak M, and Hankinson SE (2000). Plasma insulin–like growth factor (IGF) I, IGF-binding protein 3, and mammographic density. *Cancer Res* **60,** 3744–3748.

[15] Turner BC, Haffty BG, Narayanan L, Yuan J, Havre PA, Gumbs AA, Kaplan L, Burgaud JL, Carter D, Baserga R, and Glazer PM (1997). Insulin-like growth factor-I receptor overexpression mediates cellular radioresistance and local breast cancer recurrence after lumpectomy and radiation. *Cancer Res* **57,** 3079–3083.

[16] Resnik JL, Reichart DB, Huey K, Webster NJ, and Seely BL (1998). Elevated insulin-like growth factor I receptor autophosphorylation and kinase activity in human breast cancer. *Cancer Res* **58,** 1159–1164.

[17] Rocha RL, Hilsenbeck SG, Jackson JG, VanDenBerg CL, Weng C, Lee AV, and Yee D (1997). Insulin-like growth factor binding protein-3 and insulin receptor substrate-1 in breast cancer: correlation with clinical parameters and disease-free survival. *Clin Cancer Res* **3,** 103–109.

[18] Lee AV, Jackson JG, Gooch JL, Hilsenbeck SG, Coronado-Heinsohn E, Osborne CK, and Yee D (1999). Enhancement of insulin-like growth factor signaling in human breast cancer: estrogen regulation of insulin receptor substrate-1 expression *in vitro* and *in vivo*. *Mol Endocrinol* **13,** 787–796.

[19] Ethier SP, Mahacek ML, Gullick WJ, Frank TS, and Weber BL (1993). Differential isolation of normal luminal mammary epithelial cells and breast cancer cells from primary and metastatic sites using selective media. *Cancer Res* **53,** 627–635.

[20] Shi SR, Key ME, and Kalra KL (1991). Antigen retrieval in formalin-fixed, paraffin-embedded tissues: an enhancement method for immunohistochemical staining based on microwave oven heating of tissue sections. *J Histochem Cytochem* **39,** 741–748.

[21] van Golen KL, Wu ZF, Qiao XT, Bao LW, and Merajver SD (2000). RhoC GTPase, a novel transforming oncogene for human mammary epithelial cells that partially recapitulates the inflammatory breast cancer phenotype. *Cancer Res* **60,** 5832–5838.

[22] Soon LL, Yie TA, Shvarts A, Levine AJ, Su F, and Tchou-Wong KM (2003). Overexpression of WISP-1 down-regulated motility and invasion of lung cancer cells through inhibition of Rac activation. *J Biol Chem* **278,** 11465–11470.

[23] Vilmos P, Gaudenz K, Hegedus Z, and Marsh JL (2001). The Twisted gastrulation family of proteins, together with the IGFBP and CCN families, comprise the TIC superfamily of cysteine rich secreted factors. *Mol Pathol* **54,** 317–323.

[24] Kireeva ML, Mo FE, Yang GP, and Lau LF (1996). Cyr61, a product of a growth factor–inducible immediate-early gene, promotes cell proliferation, migration, and adhesion. *Mol Cell Biol* **16,** 1326–1334.

[25] Tong X, Xie D, O'Kelly J, Miller CW, Muller-Tidow C, and Koeffler HP (2001). Cyr61, a member of CCN family, is a tumor suppressor in non-small cell lung cancer. *J Biol Chem* **276,** 47709–47714.

[26] Xie D, Nakachi K, Wang H, Elashoff R, and Koeffler HP (2001). Elevated levels of connective tissue growth factor, WISP-1, and CYR61 in primary breast cancers associated with more advanced features. *Cancer Res* **61,** 8917–8923.

[27] Godden J, Leake R, and Kerr DJ (1992). The response of breast cancer cells to steroid and peptide growth factors. *Anticancer Res* **12,** 1683–1688.

[28] Jackson JG, White MF, and Yee D (1998). Insulin receptor substrate-1 is the predominant signaling molecule activated by insulin-like growth factor-I, insulin, and interleukin-4 in estrogen receptor–positive human breast cancer cells. *J Biol Chem* **273,** 9994–10003.

[29] Jackson JG, and Yee D (1999). IRS-1 expression and activation are not sufficient to activate downstream pathways and enable IGF-I growth response in estrogen receptor negative breast cancer cells. *Growth Horm IGF Res* **9,** 280–289.

[30] Peyrat JP, Bonneterre J, Dusanter-Fourt I, Leroy-Martin B, Djiane J, and Demaille A (1989). Characterization of insulin-like growth factor 1 receptors (IGF1-R) in human breast cancer cell lines. *Bull Cancer* **76,** 311–319.

[31] Satyamoorthy K, Li G, Vaidya B, Patel D, and Herlyn M (2001). Insulin-like growth factor-1 induces survival and growth of biologically early melanoma cells through both the mitogen-activated protein kinase and beta-catenin pathways. *Cancer Res* **61,** 7318–7324.

[32] Resnicoff M, and Baserga R (1998). The role of the insulin-like growth factor I receptor in transformation and apoptosis. *Ann NY Acad Sci* **842,** 76–81.

[33] Baserga R (1999). The IGF-I receptor in cancer research. *Exp Cell Res* **253,** 1–6.

[34] Santen RJ, Song RX, McPherson R, Kumar R, Adam L, Jeng MH, and Yue W (2002). The role of mitogen-activated protein (MAP) kinase in breast cancer. *J Steroid Biochem Mol Biol* **80,** 239–256.

[35] Murphy LO, Smith S, Chen RH, Fingar DC, and Blenis J (2002). Molecular interpretation of ERK signal duration by immediate early gene products. *Nat Cell Biol* **4,** 556–564.

[36] Volmat V, Camps M, Arkinstall S, Pouyssegur J, and Lenormand P (2001). The nucleus, a site for signal termination by sequestration and inactivation of p42/p44 MAP kinases. *J Cell Sci* **114,** 3433–3443.

[37] Volmat V, and Pouyssegur J (2001). Spatiotemporal regulation of the p42/p44 MAPK pathway. *Biol Cell* **93,** 71–79.

[38] Kim HS, Nagalla SR, Oh Y, Wilson E, Roberts CT Jr, and Rosenfeld RG (1997). Identification of a family of low-affinity insulin-like growth factor binding proteins (IGFBPs): characterization of connective tissue growth factor as a member of the IGFBP superfamily. *Proc Natl Acad Sci USA* **94,** 12981–12986.

[39] Burren CP, Wilson EM, Hwa V, Oh Y, and Rosenfeld RG (1999). Binding properties and distribution of insulin-like growth factor binding protein–related protein 3 (IGFBP-rP3/NovH), an additional member of the IGFBP superfamily. *J Clin Endocrinol Metab* **84,** 1096–1103.

[40] Zeslawski W, Beisel HG, Kamionka M, Kalus W, Engh RA, Huber R, Lang K, and Holak TA (2001). The interaction of insulin-like growth factor-I with the N-terminal domain of IGFBP-5. *EMBO J* **20,** 3638–3644.

Research article

Open Access

E-cadherin expression in primary carcinomas of the breast and its distant metastases

Paul J Kowalski[1], Mark A Rubin[2] and Celina G Kleer[1]

[1]Department of Pathology and Comprehensive Cancer Center, University of Michigan Medical School, Ann Arbor, Michigan, USA
[2]Department of Pathology, Brigham and Women's Hospital, Harvard Medical School, Boston, Massachusetts, USA

Correspondence: Celina G Kleer (e-mail: kleer@umich.edu)

Received: 1 Jul 2003 Revisions requested: 14 Aug 2003 Revisions received: 18 Aug 2003 Accepted: 22 Aug 2003 Published: 26 Sep 2003

Breast Cancer Res 2003, **5**:R217-R222 (DOI 10.1186/bcr651)

Abstract

Introduction Aberrant expression of E-cadherin has been associated with the development of metastases in patients with breast cancer. Even though the expression of E-cadherin has been studied in primary breast tumors, little is known about its expression at the distant metastatic sites. We investigate the relationship between E-cadherin expression in primary breast carcinoma and their distant, non-nodal metastases.

Methods Immunohistochemical analysis of E-cadherin was performed in tissues from 30 patients with primary invasive breast carcinoma and their distant metastases. E-cadherin expression was evaluated as normal or aberrant (decreased when compared with normal internal positive controls, or absent).

Results Twenty-two (73%) invasive carcinomas were ductal, and eight (27%) were lobular. Of the primary invasive ductal carcinomas, 55% (12/22) had normal E-cadherin expression and 45% (10/22) had aberrant expression. All of the metastases expressed E-cadherin with the same intensity as (12 tumors) or with stronger intensity than (10 tumors) the corresponding primaries. Of the invasive lobular carcinomas, one of eight (12%) primary carcinomas and none of the metastases expressed E-cadherin in the cell membranes, but they accumulated the protein in the cytoplasm.

Conclusion Aberrant E-cadherin expression is frequent in invasive ductal carcinomas that progress to develop distant metastases. Distant metastases consistently express E-cadherin, often more strongly than the primary tumor. Invasive lobular carcinomas have a different pattern of E-cadherin expression, suggesting a different role for E-cadherin in this form of breast carcinoma.

Keywords: breast cancer, e-cadherin, metastases

Introduction

Tumor invasion with subsequent metastases is the major cause of morbidity and mortality in patients with cancer. For patients with breast cancer, the development of metastases is the most important prognostic factor, as almost all patients with distant metastasis succumb to the disease [1–3].

Numerous studies have linked aberrant expression of E-cadherin with the development of metastases in breast cancer and other cancers. E-cadherin is a transmembrane glycoprotein that mediates calcium-dependent intercellular adhesion and is specifically involved in epithelial cell-to-cell adhesion [4–6]. The E-cadherin gene, located on chromosome 16q22.1, is an important regulator of morphogenesis [7,8]. In cancer, decreased E-cadherin expression is one of the alterations that characterizes the invasive phenotype, and the data support its role as a tumor suppressor gene [9–12]. Studies have shown that aberrant E-cadherin expression is associated with the acquisition of invasiveness and more advanced tumor stage for many cancers including lung cancer [13], prostate cancer [14,15], gastric cancer [16], colorectal carcinoma [17], and breast cancer [18–20].

Normal ductal epithelial cells in the mammary gland strongly express E-cadherin protein in the cytoplasmic membrane [21,22]. Some studies in breast cancer have

ER = estrogen receptor; PR = progesterone receptor.

demonstrated that aberrant E-cadherin expression is associated with high-grade, estrogen receptor (ER)-negative, and metastatic breast carcinomas, whereas other studies have failed to confirm these findings [22–24]. In the present article, we set out to determine and compare the expression patterns of E-cadherin in primary breast carcinomas and their distant, non-nodal metastases.

Materials and methods

Patient selection

Thirty patients with breast cancer who developed distant metastases were identified using a computerized database. Breast tissues from the primary carcinoma and the corresponding distant, non-nodal metastases were retrieved from the Surgical Pathology files in our institution, with Institutional Review Board approval.

We identified 30 cases of primary invasive breast carcinomas and 32 cases of distant metastases (two patients each had two metastatic sites). Hematoxylin and eosin stained slides were available for review in all cases. Primary invasive carcinomas were measured microscopically, and were classified as invasive ductal carcinoma, invasive lobular carcinoma or other special types according to well-accepted criteria [25,26]. A histologic grade was assigned to each primary invasive carcinoma [27].

Immunohistochemistry

E-cadherin protein expression was studied by immunohistochemistry using specific monoclonal antibodies against E-cadherin (HEC-D10; Zymed Laboratories, San Francisco, CA, USA). For assessment of ER, progesterone receptor (PR) and HER2/neu expression, specific monoclonal antibodies for ER (Ventana Medical Systems, Tucson, AZ, USA), PR (DAKO, Carpinteria, CA, USA), and HER2/neu (Herceptest; DAKO) were used following the manufacturers' recommended dilutions.

Immunohistochemistry was performed using an automated immunostainer (Biotek Techmate 500; Ventana Medical Systems) as described previously [28]. Briefly, 5 μm-thick sections were cut onto glass slides from formalin-fixed, paraffin tissue blocks. Sections were deparaffinized and were microwaved (1000 W Model #MTC1080-2A; Frigidaire, Dublin, OH, USA) in a pressure cooker (Nordic Ware, Minneapolis, MN, USA) with 1 l of 10 mM citrate buffer (pH 6.0). The sections were subsequently cooled with the lid on for an additional 10 min. After removing the lid, the entire pressure cooker was filled with cold, running tap water for 2–3 min or until the slides were cool. At 36°C, the stainer sequentially added an inhibitor of endogenous peroxidase, the primary antibodies (32 min), a biotinylated secondary antibody, an avidin–biotin complex with horseradish peroxidase, 3,3′-diaminobenzidine tetrahydrochloride, and copper enhancer. The slides were then counter-stained with hematoxylin.

Interpretation of immunohistochemical analysis

E-cadherin expression was interpreted as either normal (strong) or aberrant (reduced or absent) [29]. Internal positive controls, such as benign breast lobules and ducts, were present in most cases. Aberrant staining was defined as either negative staining or $<70\%$ membranous staining of the population of cells examined. Normal staining was defined as $\geq 70\%$ membranous staining of the cancer cells [29]. The ER and PR were considered positive when $>10\%$ of the tumor cell nuclei were stained. For HER-2/neu, the strength of the membranous staining was recorded as 0, 1+ to 3+, and a sample was considered positive when 10% or more neoplastic cells had a staining intensity of $\geq 2+$ [30].

Statistical analysis

Differences in percentages of E-cadherin-positive cases between the primary and metastatic groups were tested for statistical significance using Fisher's exact test. $P<0.05$ was considered significant. A two-sample *t* test was also performed to compare the size, the ER, PR and HER-2/neu status, and the E-cadherin expression.

Results

Clinical and pathological features

The patients' characteristics are presented in Table 1. All patients were female.

The median age at diagnosis of the primary invasive breast carcinoma was 53.9 years (range, 39–80 years). All primary tumors were treated by surgical excision. Of the primary tumors, 22 were invasive ductal carcinomas and eight were invasive lobular carcinomas. Metastatic sites included the liver (six cases), the bone marrow (five cases), the skin (four cases), the lung (three cases), the femoral head (three cases), the pelvic girdle (two cases), the vertebrae (two cases), the brain (two cases), the colon (one case), the ovary (one case), the pericardium (one case), the abdominal wall (one case), and the contralateral breast (one case).

E-cadherin expression in primary and distant metastases

Normal breast epithelial cells were used as internal positive controls for E-cadherin staining in tissue sections. The glandular epithelium consistently demonstrated unequivocal and strong membranous staining localized at the cell borders. The nonepithelial components were negative for E-cadherin protein expression. Of the invasive ductal carcinomas, 55% (12/22) had normal E-cadherin expression and 45% (10/22) had aberrant E-cadherin protein expression. Of the distant metastases of ductal carcinomas, 70% (16/23) had normal E-cadherin expression and 30% (7/23) had aberrant expression.

When we compared the staining intensity, all the metastatic cancer cells had E-cadherin expression equal to

Table 1

Clinical and pathological characteristics

Number of patients	30
Median age (range) (years)	53.9 (39–80)
Pathologic stage at diagnosis [*n* (%)]	
Stage I	3 (10)
Stage II	13 (43.3)
Stage III	6 (20)
Stage IV	2 (6.7)
Tumor size (range) (cm)	2.7 (0.5–7)
Histologic type [*n* (%)]	
Ductal	22 (73)
Lobular	8 (27)
Histologic grade [*n* (%)]	
Grade 1	6 (20)
Grade 2	17 (57)
Grade 3	7 (23)
Lymph node status [*n* (%)]	
Negative	7 (28)
Positive	18 (72)
Estrogen receptor status [*n* (%)]	
Negative	7 (27)
Positive	19 (73)
Progesterone receptor status [*n* (%)]	
Negative	9 (36)
Positive	16 (64)
Median time to develop distant metastases (months)	
Ductal	33
Lobular	74

(13/23) or stronger than (10/23) the corresponding primary tumors. Figure 1 shows a primary invasive ductal carcinoma with aberrant E-cadherin expression that developed a metastasis to the iliac bone expressing normal levels of E-cadherin (or re-expression). Figure 2 shows examples of distant metastases of invasive ductal carcinomas with normal E-cadherin expression.

Figure 2

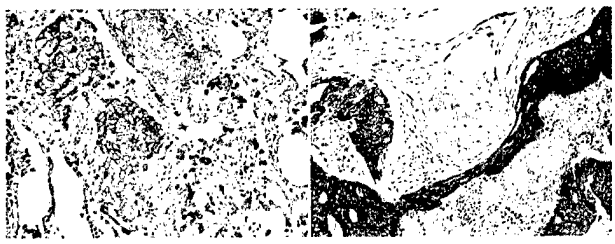

E-cadherin is expressed at normal levels at the metastatic foci. Distant metastases from two different primary invasive ductal carcinomas to **(A)** the lung and **(B)** the bone. Note the crisp membranous staining for E-cadherin, which is specific for the cancer cells. Fibroblasts and other stromal cells are negative. 200 × magnification.

All invasive lobular carcinomas (eight cases) showed cytoplasmic staining and no protein in the cellular membrane (Fig. 3). Seventy-eight percent (7/9) of metastatic lobular carcinomas showed E-cadherin protein localized to the cytoplasm of the tumor cells. The other two metastatic foci of lobular carcinoma had normal E-cadherin expression (Table 2). No association was found between E-cadherin expression in primary invasive ductal carcinomas and the ER, PR and HER-2/neu status, the histologic grade, and the tumor size.

Discussion

The expression of E-cadherin in breast cancer metastases is largely unknown and, to our knowledge, there are no studies that specifically investigate the expression of E-cadherin in primary breast carcinomas in relationship to their distant metastases. We found that aberrant E-cadherin expression is a common event in primary invasive ductal carcinomas that progress to develop distant metastases, as aberrant expression was found in 45% of these cases.

There is increasing evidence that cancer cells may re-express E-cadherin protein once they reach distant sites. We found that all the metastatic deposits from invasive ductal carcinomas expressed E-cadherin, and the

Figure 1

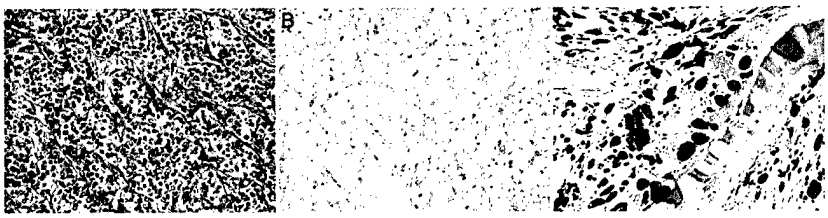

E-cadherin expression at the primary and distant metastatic sites. **(A)** and **(B)** Primary invasive ductal carcinoma with aberrant (reduced) E-cadherin expression. **(C)** This tumor metastasized 3 years later to the iliac bone. The metastatic carcinoma cells express normal levels of E-cadherin (re-expression). 200 × magnification.

Figure 3

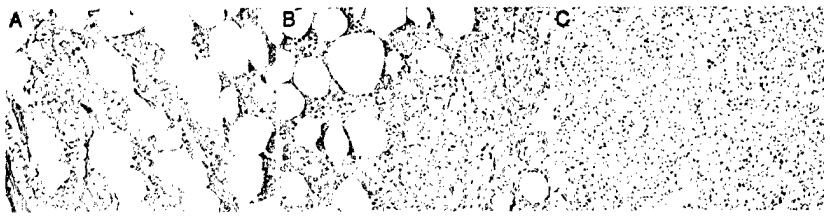

E-cadherin is accumulated in the cytoplasm of primary and metastatic lobular carcinomas of the breast. **(A)** and **(B)** Primary invasive lobular carcinoma invading fat. Notice the cellular discohesion and vacuolization typical of invasive lobular carcinomas. This tumor has cytoplasmic accumulation of E-cadherin. **(C)** Distant metastasis to the liver 8 years later exhibiting the pattern of E-cadherin expression as the primary tumor. 200 × magnification.

Table 2

E-cadherin expression in primary invasive carcinomas of the breast and their distant, non-nodal metastases

Histologic type	Total cases	Aberrant	Normal
Ductal carcinoma			
Primary tumor	22	10 (45%)	12 (55%)
Metastases	23	7 (30%)	16 (70%)
Lobular carcinoma			
Primary tumor	8	8 (100%)	0
Metastases	9	7 (78%)	2 (12%)

degree of expression was either equal to or stronger than that of the primary tumor. By studying E-cadherin expression in nodal breast cancer metastases, Bukholm and colleagues found that 19 of 20 lymph node metastases strongly expressed E-cadherin protein [21]. The mechanism and biologic role of E-cadherin re-expression at the metastatic site has not been elucidated, although it appears that translational regulation and post-translational events are probable mechanisms of E-cadherin re-expression [31].

In order to metastasize, cancer cells must break away from the primary tumor, move into the surrounding stroma, intravasate into the circulation, extravasate, and successfully re-establish growth at other sites. It is possible that loss of E-cadherin is a transient phenomenon that allows malignant cells to invade vascular channels and tissues. We have previously demonstrated that intralymphatic breast cancer emboli strongly express E-cadherin protein, and we postulate that re-expression of E-cadherin occurs in the circulating tumor cells, enabling the cancer cells to form tumor emboli and to survive [28]. E-cadherin re-expression may also enable malignant cells to form a metastatic deposit by facilitating intercellular adhesion.

The normal expression or re-expression of E-cadherin in cancer metastases appears to be similar in breast cancer and prostate cancer. Rubin and colleagues studied a large group of prostate cancers that included 77 distant metastases and detected normal E-cadherin expression in 90% of these cases [29].

In breast cancer, a relationship between E-cadherin expression and ER expression has been noted previously. ER-positive tumors have been demonstrated to express normal amounts of E-cadherin protein, and loss of ER and E-cadherin genes has been linked to disease progression in invasive carcinomas of the breast. Nass and colleagues found an association between coincident methylation of E-cadherin and the ER gene during breast cancer progression, probably not attributable to coincidence of methylation for the two genes [32]. In our study, however, we did not find an association between E-cadherin expression and the ER, PR or HER-2/neu status.

The role of E-cadherin in the pathogenesis and progression of invasive lobular carcinoma is intriguing. We found that all of the primary invasive lobular carcinomas and nearly all of the metastatic foci had accumulation of E-cadherin protein in the cytoplasm of the neoplastic cells, with no membranous staining. Several studies have demonstrated that E-cadherin is commonly downregulated in invasive lobular carcinomas [33–36]. Berx and colleagues found somatic mutations of the E-cadherin gene in 56% (27/48 cases) of invasive lobular carcinomas, and 90% of these tumors had allelic losses at the E-cadherin locus. No mutations were identified in 50 nonlobular breast cancers [34]. Sarrio and colleagues recently reported that promoter hypermethylation is another common mechanism of E-cadherin inactivation in invasive lobular carcinomas, occurring in 41% (19/46) of cases [36]. De Leeuw and colleagues reported that 84% (32/38) of invasive lobular carcinomas had completely absent membranous staining by immunohistochemistry, and 56% of these cases had staining in the cytoplasm of the cancer cells [33].

The clearly different pattern of E-cadherin expression in invasive ductal and lobular carcinomas suggests that this protein may play different roles in the development of each specific type of tumor. The absence of membranous E-cadherin expression in invasive lobular carcinomas may determine the morphologic features such as the characteristic cellular discohesion of the lobular carcinoma cells, as well as the distinct pattern of stromal invasion of invasive lobular carcinomas, typically as single cells or rows of cells.

In summary, the present study provides evidence that approximately one-half of the invasive ductal carcinomas that develop distant metastases have aberrant E-cadherin protein expression. E-cadherin is expressed or re-expressed at the distant metastatic foci of invasive ductal carcinomas, supporting the hypothesis that re-expression of E-cadherin may play a role in the establishment of the metastatic cells at distant sites. Invasive lobular carcinomas have a different pattern of E-cadherin expression both at the primary carcinoma and the metastatic sites, which suggests a different role for E-cadherin in this form of breast cancer.

Conclusion

In the present study we specifically determine the expression of E-cadherin protein in primary invasive carcinomas and their corresponding distant metastases. We conclude that E-cadherin is expressed at normal levels at the distant metastatic site regardless of the level of expression at the primary invasive ductal carcinoma. This observation may have biological implications, as re-expression of E-cadherin may allow malignant cells to form the metastatic deposits. Invasive lobular carcinomas have a different pattern of E-cadherin expression both in the primary tumor and at the metastatic site.

Competing interests

None declared.

Acknowledgements

This work was supported by DOD grant DAMD 17-02-1-0490 and DAMD 17-02-0491 (CGK), and by a grant from the John and Suzanne Munn Endowed Research Fund of the University of Michigan Comprehensive Cancer Center (CGK).

References

1. Haybittle JL, Blamey RW, Elston CW, Johnson J, Doyle PJ, Campbell FC, Nicholson RI, Griffiths K: **A prognostic index in primary breast cancer.** *Br J Cancer* 1982, **45**:361-366.
2. Rosen PR, Groshen S, Saigo PE, Kinne DW, Hellman S: **A long-term follow-up study of survival in stage I (T1N0M0) and stage II (T1N1M0) breast carcinoma.** *J Clin Oncol* 1989, **7**:355-366.
3. Danforth DN, Lichter A, Lippman ME: The diagnosis of breast cancer. In *Diagnosis and Management of Breast Cancer.* Edited by Danforth Jr DN, Lichter A, Lippman ME (Eds). Philadelphia, PA: WB Saunders; 1988:50-94.
4. Gumbiner BM: **Regulation of cadherin adhesive activity.** *J Cell Biol* 2000, **148**:399-404.
5. Deman JJ, Van Larebeke NA, Bruyneel EA, Bracke ME, Vermeulen SJ, Vennekens KM, Mareel MM: **Removal of sialic acid from the surface of human MCF-7 mammary cancer cells abolishes E-cadherin-dependent cell–cell adhesion in an aggregation assay.** *In Vitro Cell Dev Biol Anim* 1995, **31**:633-639.
6. Shore EM, Nelson WJ: **Biosynthesis of the cell adhesion molecule uvomorulin (E-cadherin) in Madin-Darby canine kidney epithelial cells.** *J Biol Chem* 1991, **266**:19672-19680.
7. Day ML, Zhao X, Vallorosi CJ, Putzi M, Powell CT, Lin C, Day KC: **E-cadherin mediates aggregation-dependent survival of prostate and mammary epithelial cells through the retinoblastoma cell cycle control pathway.** *J Biol Chem* 1999, **274**:9656-9664.
8. Peifer M: **Beta-catenin as oncogene: the smoking gun.** *Science* 1997, **275**:1752-1753.
9. Gamallo C, Palacios J, Suarez A, Pizarro A, Navarro P, Quintanilla M, Cano A: **Correlation of E-cadherin expression with differentiation grade and histological type in breast carcinoma.** *Am J Pathol* 1993, **142**:987-993.
10. Frixen UH, Behrens J, Sachs M, Eberle G, Voss B, Warda A, Lochner D, Birchmeier W: **E-cadherin-mediated cell–cell adhesion prevents invasiveness of human carcinoma cells.** *J Cell Biol* 1991, **113**:173-185.
11. Pierceall WE, Woodard AS, Morrow JS, Rimm D, Fearon ER: **Frequent alterations in E-cadherin and alpha- and beta-catenin expression in human breast cancer cell lines.** *Oncogene* 1995, **11**:1319-1326.
12. Chen WC, Obrink B: **Cell–cell contacts mediated by E-cadherin (uvomorulin) restrict invasive behavior of L-cells.** *J Cell Biol* 1991, **114**:319-327.
13. Shimoyama Y, Hirohashi S, Hirano S, Noguchi M, Shimosato Y, Takeichi M, Abe O: **Cadherin cell-adhesion molecules in human epithelial tissues and carcinomas.** *Cancer Res* 1989, **49**:2128-2133.
14. Umbas R, Isaacs WB, Bringuier PP, Schaafsma HE, Karthaus HF, Oosterhof GO, Debruyne FM, Schalken JA: **Decreased E-cadherin expression is associated with poor prognosis in patients with prostate cancer.** *Cancer Res* 1994, **54**:3929-3933.
15. Umbas R, Isaacs WB, Bringuier PP, Xue Y, Debruyne FM, Schalken JA: **Relation between aberrant alpha-catenin expression and loss of E-cadherin function in prostate cancer.** *Int J Cancer* 1997, **74**:374-377.
16. Mayer B, Johnson JP, Leitl F, Jauch KW, Heiss MM, Schildberg FW, Birchmeier W, Funke I: **E-cadherin expression in primary and metastatic gastric cancer: down-regulation correlates with cellular dedifferentiation and glandular disintegration.** *Cancer Res* 1993, **53**:1690-1695.
17. Dorudi S, Hanby AM, Poulsom R, Northover J, Hart IR: **Level of expression of E-cadherin mRNA in colorectal cancer correlates with clinical outcome.** *Br J Cancer* 1995, **71**:614-616.
18. Rasbridge SA, Gillett CE, Sampson SA, Walsh FS, Millis RR: **Epithelial (E-) and placental (P-) cadherin cell adhesion molecule expression in breast carcinoma.** *J Pathol* 1993, **169**:245-250.
19. Oka H, Shiozaki H, Kobayashi K, Inoue M, Tahara H, Kobayashi T, Takatsuka Y, Matsuyoshi N, Hirano S, Takeichi M: **Expression of E-cadherin cell adhesion molecules in human breast cancer tissues and its relationship to metastasis.** *Cancer Res* 1993, **53**:1696-1701.
20. Palacios J, Benito N, Pizarro A, Suarez A, Espada J, Cano A, Gamallo C: **Anomalous expression of P-cadherin in breast carcinoma. Correlation with E-cadherin expression and pathological features.** *Am J Pathol* 1995, **146**:605-612.
21. Bukholm IK, Nesland JM, Borresen-Dale AL: **Re-expression of E-cadherin, alpha-catenin and beta-catenin, but not of gamma-catenin, in metastatic tissue from breast cancer patients [see comments].** *J Pathol* 2000, **190**:15-19.
22. Bukholm IK, Nesland JM, Karesen R, Jacobsen U, Borresen-Dale AL: **E-cadherin and alpha-, beta-, and gamma-catenin protein expression in relation to metastasis in human breast carcinoma.** *J Pathol* 1998, **185**:262-266.
23. Jones JL, Royall JE, Walker RA: **E-cadherin relates to EGFR expression and lymph node metastasis in primary breast carcinoma.** *Br J Cancer* 1996, **74**:1237-1241.
24. Moll R, Mitze M, Frixen UH, Birchmeier W: **Differential loss of E-cadherin expression in infiltrating ductal and lobular breast carcinomas.** *Am J Pathol* 1993, **143**:1731-1742.

25. Rosen PP, Oberman HA: *Tumors of the Mammary Gland. Atlas of Tumor Pathology.* Washington, DC: Armed Forces Institute of Pathology; 1993.
26. Tavassoli F: **General considerations in breast pathology.** In *Breast Pathology.* Edited by Tavassoli F. Connecticut: Appelton & Lange, 1999:27-74.
27. Elston CW, Ellis IO: **Pathological prognostic factors in breast cancer. I. The value of histological grade in breast cancer: experience from a large study with long-term follow-up.** *Histopathology* 1991, **19**:403-410.
28. Kleer CG, van Golen KL, Braun T, Merajver SD: **Persistent E-cadherin expression in inflammatory breast cancer.** *Mod Pathol* 2001, **14**:458-464.
29. Rubin MA, Mucci NR, Figurski J, Fecko A, Pienta KJ, Day ML: **E-cadherin expression in prostate cancer: a broad survey using high-density tissue microarray technology.** *Hum Pathol* 2001, **32**:690-697.
30. Seidman AD, Fornier MN, Esteva FJ, Tan L, Kaptain S, Bach A, Panageas KS, Arroyo C, Valero V, Currie V, Gilewski T, Theodoulou M, Moynahan ME, Moasser M, Sklarin N, Dickler M, D'Andrea G, Cristofanilli M, Rivera E, Hortobagyi GN, Norton L, Hudis CA: **Weekly trastuzumab and paclitaxel therapy for metastatic breast cancer with analysis of efficacy by HER2 immunophenotype and gene amplification.** *J Clin Oncol* 2001, **19**:2587-2595.
31. Rashid MG, Sanda MG, Vallorosi CJ, Rios-Doria J, Rubin MA, Day ML: **Posttranslational truncation and inactivation of human E-cadherin distinguishes prostate cancer from matched normal prostate.** *Cancer Res* 2001, **61**:489-492.
32. Nass SJ, Herman JG, Gabrielson E, Iversen PW, Parl FF, Davidson NE, Graff JR: **Aberrant methylation of the estrogen receptor and E-cadherin 5′ CpG islands increases with malignant progression in human breast cancer.** *Cancer Res* 2000, **60**: 4346-4348.
33. De Leeuw WJ, Berx G, Vos CB, Peterse JL, Van de Vijver MJ, Litvinov S, Van Roy F, Cornelisse CJ, Cleton-Jansen AM: **Simultaneous loss of E-cadherin and catenins in invasive lobular breast cancer and lobular carcinoma in situ.** *J Pathol* 1997, **183**:404-411.
34. Berx G, Cleton-Jansen AM, Nollet F, de Leeuw WJ, van de Vijver M, Cornelisse C, van Roy F: **E-cadherin is a tumour/invasion suppressor gene mutated in human lobular breast cancers.** *Embo J* 1995, **14**:6107-6115.
35. Berx G, Cleton-Jansen AM, Strumane K, de Leeuw WJ, Nollet F, van Roy F, Cornelisse C: **E-cadherin is inactivated in a majority of invasive human lobular breast cancers by truncation mutations throughout its extracellular domain.** *Oncogene* 1996, **13**: 1919-1925.
36. Sarrio D, Moreno-Bueno G, Hardisson D, Sanchez-Estevez C, Guo M, Herman JG, Gamallo C, Esteller M, Palacios J: **Epigenetic and genetic alterations of APC and CDH1 genes in lobular breast cancer: relationships with abnormal E-cadherin and catenin expression and microsatellite instability.** *Int J Cancer* 2003, **106**:208-215.

Correspondence

Celina G Kleer, MD, Department of Pathology, 2G332 University Hospital, 1500 East Medical Center Drive, Ann Arbor, MI 48109-0054, USA. Tel: +1 734 936 6775; fax: +1 734 763 4095; e-mail: kleer@umich.edu

EZH2 is a marker of aggressive breast cancer and promotes neoplastic transformation of breast epithelial cells

Celina G. Kleer*†‡§, Qi Cao*‡, Sooryanarayana Varambally*‡, Ronglai Shen*¶, Ichiro Ota†‖, Scott A. Tomlins*, Debashis Ghosh†¶, Richard G. A. B. Sewalt**, Arie P. Otte**, Daniel F. Hayes†‖, Michael S. Sabel†,††, Donna Livant†‡‡, Stephen J. Weiss†‖, Mark A. Rubin§§, and Arul M. Chinnaiyan*†§¶¶

Departments of *Pathology, ¶Biostatistics, ‖Internal Medicine, ††Surgery, ‡‡Radiation Oncology, and ¶¶Urology, and †Comprehensive Cancer Center, University of Michigan Medical School, Ann Arbor, MI 48109; **Swammerdam Institute for Life Sciences, Biocentrum Amsterdam, University of Amsterdam, 1018 TV Amsterdam, The Netherlands; and §§Department of Pathology, Brigham and Women's Hospital, Harvard Medical School, Boston, MA 02115

Edited by Lawrence H. Einhorn, Indiana University, Indianapolis, IN, and approved July 28, 2003 (received for review June 19, 2003)

The Polycomb Group Protein EZH2 is a transcriptional repressor involved in controlling cellular memory and has been linked to aggressive prostate cancer. Here we investigate the functional role of EZH2 in cancer cell invasion and breast cancer progression. EZH2 transcript and protein were consistently elevated in invasive breast carcinoma compared with normal breast epithelia. Tissue microarray analysis, which included 917 samples from 280 patients, demonstrated that EZH2 protein levels were strongly associated with breast cancer aggressiveness. Overexpression of EZH2 in immortalized human mammary epithelial cell lines promotes anchorage-independent growth and cell invasion. EZH2-mediated cell invasion required an intact SET domain and histone deacetylase activity. This study provides compelling evidence for a functional link between dysregulated cellular memory, transcriptional repression, and neoplastic transformation.

Breast cancer is a leading cause of cancer-related death in women, accounting for ≈40,000 deaths per year in the United States (1). Despite advances in the early detection and treatment of breast cancer, mortality for those 20% of patients with recurrences and or metastases is ≈100% (2). Currently, the most important prognostic markers for patients with breast cancer that are used in the clinical setting are components of the staging system, such as primary tumor size and the presence of lymph node metastasis (3). However, the accuracy of these conventional indicators is not as precise as desired, leading to inefficient application of systemic therapy (4). Thus, there is a need for novel molecular predictors of tumor behavior at the time of diagnosis that will help guide clinical therapy decisions.

Few biomarkers of breast cancer progression have been proven to be clinically useful (4). Estrogen receptor (ER) and progesterone receptor (PR) are highly predictive of breast cancer patients that will benefit from endocrine therapy (5) but are weak prognostic factors (6). Other tumor markers that have been considered for prognostication in breast cancer include erbB2 amplification/overexpression, cathepsin D, and uPAR (4). The consensus, however, remains that new prognostic factors that are more precise and reliable are needed (7).

Through our gene expression profiling studies, we identified EZH2 as being overexpressed in metastatic prostate cancer (8). In clinically localized prostate cancer, EZH2 was found to be predictive of poor outcome postprostatectomy (i.e., biochemical recurrence or metastasis). EZH2 is a Polycomb Group (PcG) protein homologous to *Drosophila* Enhancer of Zeste and involved in gene silencing (9, 10). PcG proteins are presumed to function in controlling the transcriptional memory of a cell (9). Dysregulation of this gene silencing machinery can lead to cancer (9, 11, 12). In the context of prostate cancer, we provided evidence that EZH2 functions as a transcriptional repressor, and inhibition of EZH2 blocks prostate cell growth (8). Interestingly, several recent studies demonstrated that EZH2 has enzymatic activity and functions as a histone H3 methyltransferase (13–15).

Biochemical analysis indicates that PcG proteins belong to at least two multimeric complexes, PRC1 (16) and EED-EZH2 (Enx1) (17). These complexes are thought to heritably silence genes by acting at the level of chromatin structure. The EED protein interacts directly with type 1 histone deacetylases (HDACs) in mammalian cells (18), and in *Drosophila* (19), and this has been suggested to be part of the silencing mechanism. Furthermore, recent studies have demonstrated that EED/EZH2 complexes methylate H3-K9 and K27 *in vitro*, with a strong preference for K27 (13–15). Methylation of both H3-K9 (20) and H3-K27 is thought to be involved in targeting the PRC1 complex to specific genetic target loci.

By interrogating publicly available gene expression data sets, we identified EZH2 as being dysregulated in breast cancer. In the present study, we examined EZH2 mRNA transcript and protein level in normal breast and in breast cancer progression. Immunohistochemical analyses performed on a spectrum of breast cancer specimens demonstrated that high EZH2 levels were strongly associated with poor clinical outcome in breast cancer patients. EZH2 was an independent predictor of breast cancer recurrence and death and provided prognostic information above and beyond known clinical, pathologic, and biomarkers studied. Overexpression of EZH2 in normal breast epithelial cell lines produced a neoplastic phenotype characterized by anchorage-independent growth and cell invasion. Neoplastic transformation mediated by EZH2 depended on both the SET domain as well as HDAC activity. Importantly, we propose a biologic basis for the association of EZH2 and tumor aggressiveness in that high levels of EZH2 promote the invasive potential of carcinomas.

Methods

Selection of Patients and Tissue Microarray Development. Breast tissues for tissue microarray construction were obtained from the Surgical Pathology files at the University of Michigan with Institutional Review Board approval. A total of 280 cases (n = 917 tissue microarray samples) were reviewed by the study pathologist (C.G.K.) and arrayed in three high-density tissue microarrays, as described (21, 22). See *Supporting Methods*, which are published as supporting information on the PNAS web site, www.pnas.org, for details.

This paper was submitted directly (Track II) to the PNAS office.

Abbreviations: ER, estrogen receptor; PR, progesterone receptor; PcG, Polycomb Group; HDAC, histone deacetylase; TSA, trichostatin A; ECM, extracellular membrane; SU, sea urchin; CAM, chicken chorioallantoic membrane; SAHA, suberoylanilide hydroxamic acid.

‡C.G.K., Q.C., and S.V. contributed equally to this work.

§To whom correspondence may be addressed. E-mail: kleer@umich.edu or arul@umich.edu.

www.pnas.org/cgi/doi/10.1073/pnas.1933744100

Immunohistochemical Studies. Immunohistochemistry was performed on the tissue microarrays (TMAs) by using standard biotin–avidin complex technique and a polyclonal antibody against EZH2 that was previously validated by immunoblot analysis (8). See *Supporting Methods* for detailed methodology. The TMAs were immunostained for ER and PR and for HER-2/neu by using well described and validated procedures (23). See *Supporting Methods* for details.

Statistical Analysis. Comparison of the intensity of EZH2 staining between normal breast, hyperplasia, ductal carcinoma *in situ*, invasive carcinoma, and metastases was carried out by calculating the median staining intensity for each case and applying the Wilcoxon rank test. A P value of <0.05 was considered significant. Overall survival was calculated from the date of surgical excision of the primary tumor to the date of death. Patients who died of or with the disease were included in the analysis. For disease-specific survival, data for patients who died from other causes were censored at the time of death. Overall survival and disease-specific survival curves were constructed by the Kaplan–Meier method. Clinical criteria for treatment failure were local recurrence and/or the development of metastases.

Univariate analyses of disease-specific survival were performed by using a two-sided log-rank test to evaluate EZH2 protein expression, age, tumor size, nodal status, stage, angiolymphatic invasion, ER status, PR status, and HER-2/neu status. To assess the influence of several variables simultaneously, a multivariable Cox proportional hazards model of statistically significant covariates was developed by removing nonsignificant parameters in a step-wise manner. Statistical significance in the Cox models was determined by Wald's test.

SYBR Green Quantitative Real-Time PCR. We performed SYBR green real-time quantitative PCR analysis on 19 laser-microdissected frozen breast tissues obtained from the frozen breast tissue bank in our institution with Institutional Review Board approval. See *Supporting Methods* for details.

Immunoblot Analysis. Protein extracts were prepared from normal and cancerous breast tissues and standard immunoblot analysis performed. See *Supporting Methods* for details.

Adenovirus Constructs. Adenoviral constructs were generated by *in vitro* recombination. In brief, the full-length EZH2 or SET domain deleted EZH2 (EZH2ΔSET) were inserted in an adenoviral shuttle plasmid [pACCMVpLpA(−)loxP-SSP]. Viruses were generated by transfection into the 293-complementation cell line. Virus was propagated in 911 cells and purified on a CsCl gradient. Multiplicities of infection were calculated, and purified viruses were stored in 10 mM Tris·HCl (pH 7.4)/137 mM NaCl/5 mM KCl/1 mM MgCl2 in 10% glycerol (by volume).

Cell Count. H16N2 were infected with EZH2 adenovirus. Cell counts were estimated by trypsinizing cells and analysis by Coulter counter at the indicated time points in triplicate.

Soft Agar Assay. A 0.6% (wt/vol) bottom layer of low melting point agarose in normal medium was prepared in six-well culture plates. On top, a layer of 0.6% agarose containing 1×10^5 stable transfected cells was placed (24). After 25 days, foci were stained with P-Iodonitrotetrazolium violet and counted.

HDAC Assay. HDAC activity assays were performed according to the manufacturer's instructions (Biomol, Plymouth Meeting, PA). See *Supporting Methods* for details.

Basement Membrane Matrix Invasion Assay. Cells were infected with vector, EZH2, and EZH2ΔSET adenovirus. Forty-eight hours after infection, the cells were trypsinized and seeded at equal numbers onto the basement membrane matrix 24-well culture plates [extracellular membrane (ECM); Chemicon] in the presence or absence of HDAC inhibitors suberoylanilide hydroxamic acid (SAHA) (7.5 μM) and trichostatin A (TSA) (0.5 μM). FBS was added to the lower chamber to act as a chemoattractant. After 48-h incubation, the noninvading cells and ECM were removed gently by cotton swab. The cells that are invaded that are present on the lower side of the chamber were stained, air dried, and photographed. The invaded cells were counted under the microscope. For colorimetric assay, the inserts were treated with 150 μl of 10% acetic acid, and absorbance was measured at 560 nm.

Sea Urchin (SU) Embryo Basement Membrane Invasion Assay. H16N2 cells were infected with vector, EZH2, and EZH2ΔSET adenovirus and trypsinized after 48 h. The infected cells alone or treated with HDAC inhibitors SAHA (7.5 μM) and TSA (0.5 μM) and analyzed for invasiveness by using the SU embryo basement membrane invasion assay (25). See *Supporting Methods* for details.

Chick Chorioallantoic Membrane (CAM) Invasion Assay. EZH2- and control virus-infected H16N2 cells were labeled with Fluoresbrite carboxylated polystyrene nanospheres of 48 nm diameter (Polysciences) as described (26). See *Supporting Methods* for details.

Results

EZH2 Transcript and Protein Expression Are Elevated in Breast Cancer. On the basis of our previous work characterizing EZH2 in prostate cancer (8), we were interested in determining whether EZH2 is dysregulated in breast cancer, which, similar to prostate cancer, is steroid hormone regulated. This was facilitated by our group's ongoing efforts to create a cancer microarray metaanalysis database (see www.ONCOMINE.org) stemming from our initial work in prostate (27). Of the five publicly available breast cancer gene expression datasets (28–32), only the Perou *et al.* (28) study had neoplastic and normal breast tissues to make comparisons between benign and cancer. Interestingly, in this dataset, we found that the EZH2 transcript was overexpressed significantly in invasive breast cancer and metastatic breast cancer relative to normal ($P = 0.002$, t test) (28).

To validate these DNA microarray results, we carried out SYBR green quantitative real-time PCR on 19 laser-capture microdissected normal and invasive breast cancers. As predicted, levels of EZH2 mRNA were increased an average of 7.5-fold in invasive carcinomas compared with normal breast epithelial cells (t test, $P = 0.0085$) (Fig. 1*a*). To confirm that EZH2 is elevated at the protein level in invasive breast cancer, we analyzed normal breast and breast cancer tissue extracts by immunoblot analysis. Consistent with the transcript data, invasive breast cancer expressed high levels of EZH2 protein relative to normal (Fig. 1*b*). Importantly, EED, a PcG protein that forms a complex with EZH2, did not exhibit similar protein dysregulation.

Using high-density tissue microarrays, we next evaluated the expression of EZH2 protein in a wide range of breast tissues (280 patients, $n = 917$ samples) to characterize its expression *in situ* by immunohistochemistry. EZH2 protein expression was observed primarily in the nucleus (Fig. 1*c*), as reported previously (33). Invasive breast cancer that expressed high levels of EZH2 (scores 3–4, EZH2+) and those that expressed low levels of EZH2 (scores 1–2, EZH2−) were readily apparent (Fig. 1*c Center* and *Right*). There was a remarkable staining difference between tumor cells that form intravascular emboli and adjacent normal breast epithelia (Fig. 1*c Left*). Consistent with our mRNA transcript data, EZH2 protein levels were elevated in invasive carcinoma relative to normal or atypical hyperplasia (Wilcoxon test, $P < 0.0001$, Fig. 1*d*). As in the case of metastatic prostate cancer (8), breast cancer metastases expressed high levels of EZH2 (Fig. 1*d*). Median EZH2 staining intensities of normal, atypical hyperplasia, ductal carcinoma *in situ* (DCIS), invasive carcinoma, and metastases were 1.47 (SE 0.61), 2 (SE 0), 2.38 (SE 0.52), 2.74 (SE 0.99), and 3.09 (SE 1.04), respectively (Fig. 1*d*). Interestingly, increased EZH2 protein and transcript were already present in DCIS, a precursor of invasive carcinoma (Fig. 1*d*).

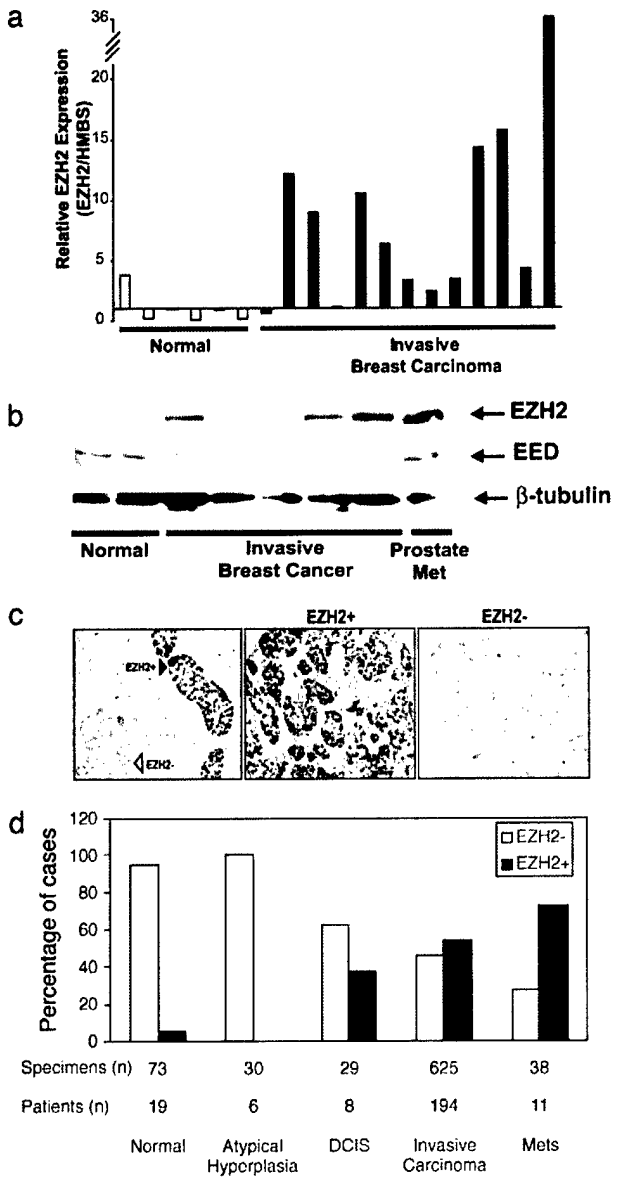

Fig. 1. EZH2 mRNA transcript and protein levels are elevated in breast cancer. (*a*) Quantitative SYBR green RT-PCR of EZH2 transcript in laser-capture microdissected normal and breast cancer epithelia. Each sample was performed in duplicate, and a ratio was calculated relative to the housekeeping gene hydroxymethylbilane synthase (HMBS). (*b*) Immunoblot analysis of EZH2 and EED in breast tissue extracts. Metastatic (Met) prostate cancer was used as a positive control. β-Tubulin was included as a loading control. (*c*) Representative breast tissue sections stained with an antibody to EZH2. (*Left*) Normal breast epithelia (open triangle) and adjacent intravascular breast cancer emboli (filled triangle). (*Center*) An invasive breast cancer expressing high levels of EZH2. (*Right*) An invasive breast cancer expressing low levels of EZH2. (*d*) Tissue microarray analysis of EZH2 expression in breast cancer progression. Tumor specimens were stratified into high EZH2 expressors (filled bars, scored 3 or 4) and low EZH2 expressors (open bars, scored 1 or 2). The *y* axis represents the percentage of patients in each category.

Prognostic Value of EZH2 in Breast Cancer. To investigate whether EZH2 mRNA expression levels are associated with outcome, we analyzed the published van't Veer *et al.* (30) breast cancer gene expression dataset, which contains outcome information on 78 sporadic invasive carcinomas <5 cm with negative lymph nodes. We found that the levels of EZH2 transcript expression were significantly higher in invasive carcinomas that metastasized within 5 years of primary diagnosis when compared with invasive carcinomas that did not metastasize (Wilcoxon rank test $P = 0.01$, Fig. 2*a*). By Kaplan–Meier analysis, high EZH2 expression [>1.26 (log10 ratio >0.1)] was associated significantly with the development of metastasis within 5 years of primary diagnosis (log rank $P < 0.0001$). Multivariable Cox hazards regression analysis showed that EZH2 mRNA expression was an independent predictor of the development of metastases with a hazard ratio of 2.02 (95% confidence interval 1.08–3.76, $P = 0.03$).

By using our breast cancer tissue microarray data, we were in the position to evaluate clinical and pathology associations of EZH2 protein levels in breast cancer. In our cohort of 236 consecutive breast cancer patients ($n = 712$ samples), 194 had complete follow-up information. Clinicopathologic characteristics of the patients can be found in Table 1. The median age of the study population was 56 years (ranging from 26 to 89 years). After a median follow-up of 3.2 years (range 17 days to 15.8 years), 42 of the 194 patients (21.6%) died of breast cancer. The 5- and 10-year disease-specific survival rates for the entire cohort of patients were 60.28% and 38.66%, respectively. The association between EZH2 protein levels and clinical characteristics is shown in Table 3, which is published as supporting information on the PNAS web site. EZH2 expression was strongly associated with standard pathology predictors of clinical outcome, including tumor diameter ($P = 0.002$) and stage of disease ($P < 0.0001$). Higher EZH2 levels were also significantly associated with decreasing age ($P = 0.0003$), negative ER status ($P = 0.0001$), negative PR status ($P < 0.0001$), and lymph node status ($P = 0.001$), but not HER2/neu overexpression. Hazard ratios of recurrence or metastasis according to EZH2 status were 2.92 ($P < 0.0001$).

The results of the univariate analysis are shown in Table 4, which is published as supporting information on the PNAS web site. As expected, at the univariate level, lymph node status, tumor diameter, and stage of disease were associated with disease-specific and overall survival. Hormone receptor status was inversely associated with outcome. We found a strong association between EZH2 protein levels and patient outcome. Higher EZH2 protein levels were associated with a shorter disease-free interval after initial surgical treatment, lower overall survival, and a high probability of disease-specific death (or death due to breast cancer) (Fig. 2 *b* and *c*). The 10-year disease-free survival for patients with tumors expressing high EZH2 levels was 24.76% and, by contrast, 58.92% for low levels of EZH2 (log rank $P < 0.0001$, Fig. 2*b*). High EZH2 expression was associated with disease-specific survival in patients with lymph node-negative disease (log rank $P = 0.007$). EZH2 expression was associated with disease-specific survival in patients with stage I and II disease (log rank, $P = 0.037$ and $P = 0.048$, respectively), but not in patients with advanced stage (stages III and IV). EZH2 was not associated with survival in patients with positive lymph nodes. The strong inverse association between high EZH2 protein expression and negative ER status (Kruskal–Wallis test, $P = 0.001$, Table 3) prompted us to investigate whether the prognostic utility of EZH2 depends on ER status. Kaplan–Meier analysis showed that EZH2 levels were strongly associated with outcome in both ER-positive and -negative invasive carcinomas (see Fig. 5, which is published as supporting information on the PNAS web site). Thus, our data suggest that EZH2 has prognostic utility independently of ER status.

The best multivariable model predictive of disease-specific survival included positive lymph nodes, high EZH2 expression, and negative PR status (Table 2). High EZH2 expression was a strong independent predictor of outcome providing survival information above other independent prognostic features, with a hazard ratio of 2.04 and a 95% confidence interval of 1.17–3.57, $P = 0.01$. Tumor size, angiolymphatic invasion, and ER status, identified as having strong associations with EZH2 at the univariate level, were not independently associated with outcome at the multivariable level.

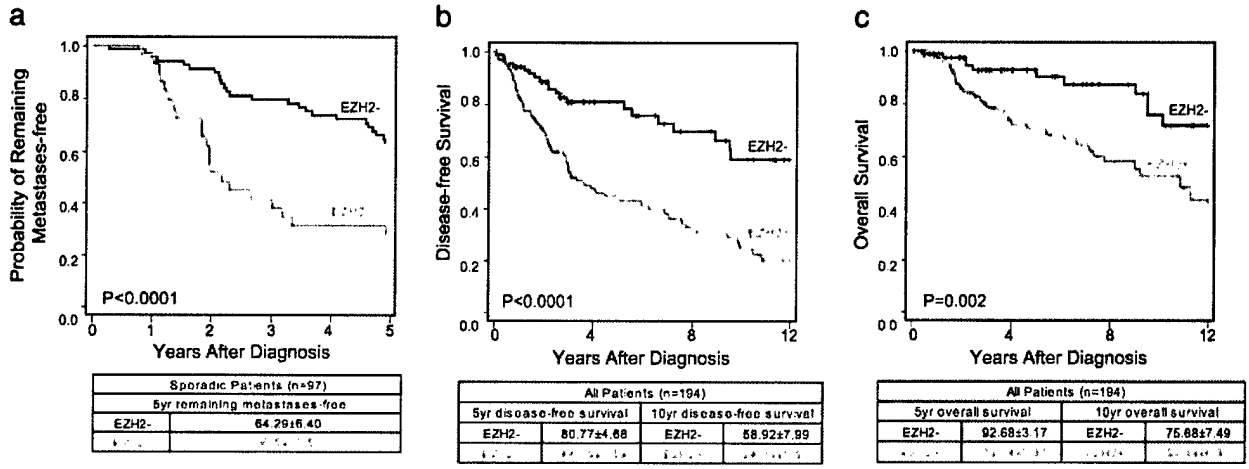

Fig. 2. High EZH2 levels are associated with aggressive breast cancer. (*a*) Kaplan–Meier analysis of metastasis-free survival according to EZH2 mRNA transcript levels as measured using DNA microarrays by van't Veer *et al.* (30). Kaplan–Meier analysis of disease-specific (*b*) and overall (*c*) survival according to EZH2 protein levels as assessed by immunohistochemical analysis. Patients grouped on the basis of high (+) or low (−) EZH2 expression levels. *P* values were calculated by using the log-rank test.

EZH2 Overexpression Promotes Anchorage-Independent Growth and HDAC Activity in Normal Breast Epithelial Cells. To study the function of dysregulated EZH2 expression in breast epithelial cells, we generated adenovirus constructs expressing EZH2. We also generated an adenovirus expressing a mutant version of EZH2 in which the C-terminal SET domain is truncated (EZH2ΔSET). Normal immortalized breast epithelial cells (H16N2) (34) were infected with EZH2 and EZH2ΔSET expressing viruses and protein expression demonstrated in Fig. 3*a*. Overexpression of EZH2 in breast epithelial cells did not significantly enhance cell proliferation in tissue culture (Fig. 3*b*). Interestingly, EZH2 overexpression markedly promoted colony formation in soft agar relative to EZH2ΔSET and vector controls (Fig. 3 *c* and *d*). In fact, colonies were present only in EZH2-infected H16N2 cells, supporting the notion that EZH2 can facilitate anchorage-independent growth. As in our previous study with prostate cells (8), overexpression of EZH2 in breast carcinoma cells induced transcriptional repression of a cohort of target genes (data not shown). Previous studies have demonstrated that the EED–EZH2 complex recruits type I HDACs (18). To determine whether overexpression of EZH2 modulates HDACs, we measured HDAC enzymatic activity in breast epithelial cell lysates. Overexpression of EZH2 but not the EZH2ΔSET mutant increased total HDAC activity in breast epithelial cells. This activity was completely abrogated in the presence the HDAC inhibitor TSA.

Dysregulated EZH2 Orchestrates the Invasive Potential of Breast Epithelial Cells. We next assessed the biological function of EZH2 in the context of cancer cell invasion. We observed that overexpression of EZH2 in breast epithelial cells promotes invasion in a reconstituted basement membrane invasion chamber assay (Fig. 4 *a* and *b*). The control experiments that included EZH2ΔSET mutant and vector did not exhibit similar proinvasive properties. Importantly, EZH2-mediated invasion was attenuated with inclusion of the HDAC inhibitors TSA and SAHA. Cell invasion was quantitated by both cell counting and colorimetry (Fig. 4*b*). Next, we used SU-ECM (25, 35) as invasion substrates to examine the invasive properties of EZH2 expressing breast epithelial cells. The SU-ECM assay has advantages over the reconstituted basement membrane assay in that it is a uniform, biological, serum-free basement membrane that closely mimics the type of extracellular matrix that cells encounter *in vivo*. As with the reconstituted basement membrane assay, EZH2 overexpression in the SU-ECM assay supported similar findings regarding the invasive potential of EZH2 and its requirement for HDAC activity (Fig. 4*c*).

To examine the role of EZH2-mediated invasion in an *in vivo* setting, we used a CAM assay. In this model, EZH2 overexpressing breast epithelial cells are labeled with fluorescent beads, seeded in duplicate on CAMs, of 10-day-old chicken embryos and incubated. At time of harvest, frozen sections were made from the CAM tissues and examined by fluorescent and light microscopy after hematoxylin/eosin staining. EZH2 overexpressing breast epithelial

Table 1. Demographics of patients with clinical follow-up used in this study

Parameter	Value
No. of patients	194
Median age, years (range)	56 (26–89)
Follow-up/years, median (range)	3.2 years (17 d–16 years)
Pathologic stage, no. (%)	
I	78 (40)
II	66 (34)
III	32 (16)
IV	18 (10)
Tumor size, cm (range)	2 (0.3–6.7)
Lymph node status, no. (%)	
Negative	99 (56)
Positive	78 (44)
ER status	
Negative, no. (%)	67 (36)
Positive, no. (%)	120 (64)
PR status	
Negative, no. (%)	86 (45)
Positive, no. (%)	107 (55)
HER-2/neu status	
Negative, no. (%)	163 (85)
Positive, no. (%)	28 (15)

Table 2. Independent factors predictive of death from breast cancer

Parameter	*P* value	Hazard ratio	95% confidence interval for hazard ratio	
EZH2 positive (vs. negative)	0.01	2.04	1.17	3.57
Positive lymph nodes (≥4, 1–3, 0)	<0.0001	1.9	1.4	2.57
PR positive (vs. negative)	0.02	0.54	0.32	0.91

Multivariate Cox Model with backward selection, $n = 161$, $P < 0.0001$ disease-free survival.

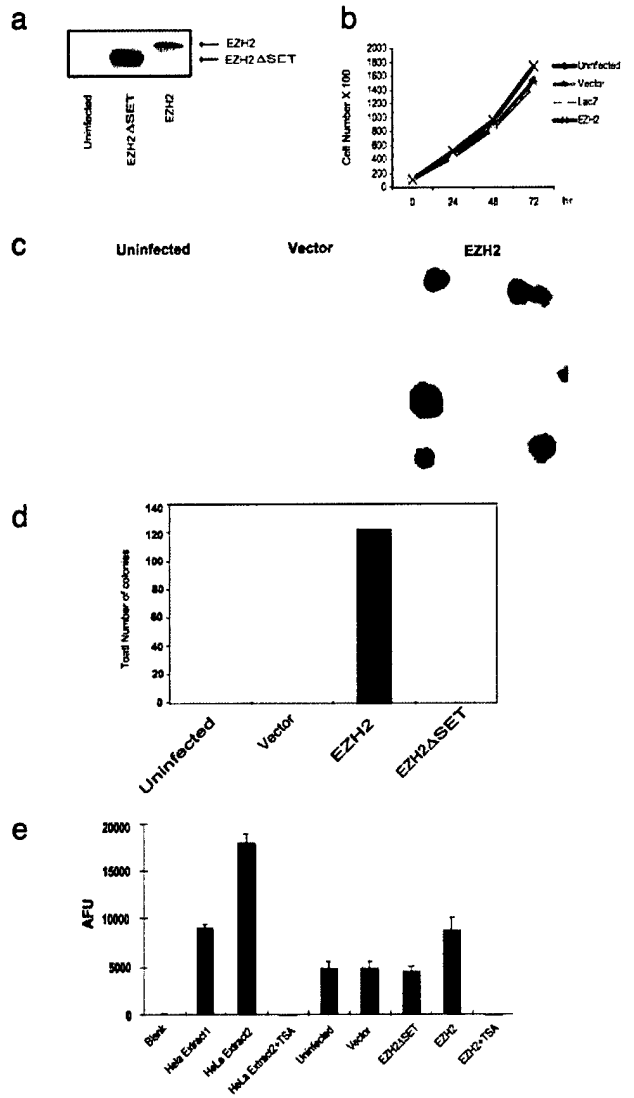

Fig. 3. Anchorage-independent growth mediated by EZH2. (*a*) Immunoblot analysis of breast cell line H16N2 infected with adenovirus encoding EZH2 or EZH2 Δ SET mutant. (*b*) Ectopic overexpression of EZH2 does not significantly enhance growth of breast epithelial cells in culture. H16N2 cells were infected with EZH2 adenovirus and controls, and cells were counted at indicated time points. LacZ adenovirus and vector adenovirus were used as controls. (*c*) EZH2 expression enhances anchorage-independent growth *in vitro*. H16N2 cells were infected with EZH2, EZH2 Δ SET, or vector adenoviruses. Anchorage-independent growth was determined by assaying colony formation in soft agar as described in *Methods*. After 25 days, the plates were stained and photographed. (*d*) Quantitation of soft agar colonies from experiments described in c. Colonies from three wells were quantitated for each condition. (e) EZH2 induces HDAC activity in breast epithelial cells. HDAC activity was measured in extracts from H16N2 cells infected with indicated viruses ± treatment with TSA (1.0 μM). As indicated by the manufacturer (Biomol), nuclear extracts from HeLa cells were used as positive controls. Extract 2 had 2-fold more HDAC activity than Extract 1. AFU, arbitrary fluorescence units.

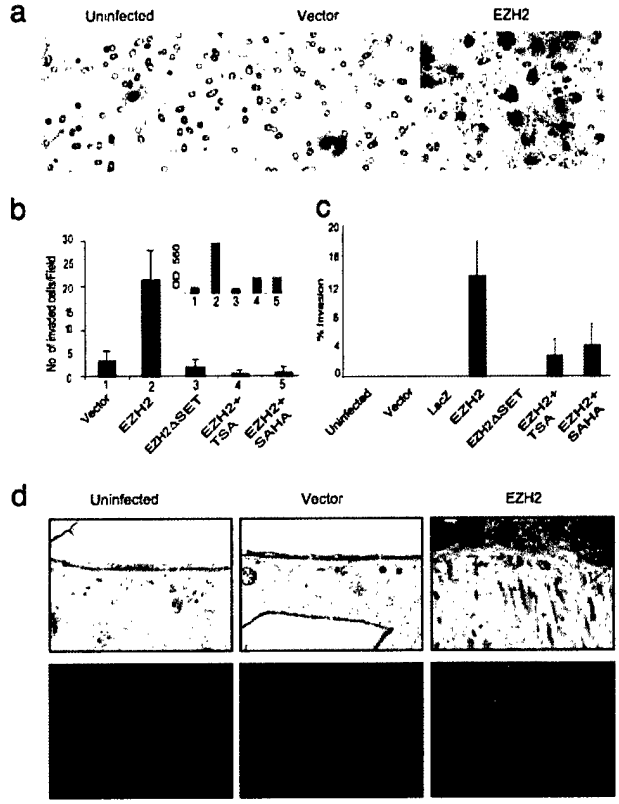

Fig. 4. EZH2 orchestrates cell invasion both *in vitro* and *in vivo*. (*a*) A reconstituted basement membrane invasion chamber assay (Chemicon) was used to assess breast epithelial cell lines infected with EZH2 and control adenoviruses. Representative fields of invaded and stained cells are shown. (*b*) The numbers of invaded cells were counted in six fields, and the mean values were determined. Quantitation by colorimetry (absorbance at 560 nm) is shown in *Inset*. (c) EZH2-mediated invasion of SU-ECM. H16N2 cells were infected with EZH2, EZH2 Δ SET, or control adenoviruses. (*d*) EZH2 overexpression mediates invasion of breast epithelial cells in a CAM assay. (*Upper*) CAM tissues stained with hematoxylin/eosin. Arrows indicate the cells that have invaded the CAM. Because cells were labeled with Fluoresbrite carboxylated polystyrene nanospheres, they could also be visualized by fluorescence (*Lower*).

cells consistently promoted invasion of the CAM (a representative experiment is shown in Fig. 4*d*).

Discussion

In the present study, we characterized the expression pattern of EZH2 transcript and protein in a wide spectrum of breast disease and assessed the utility of EZH2 as a prognostic marker in patients with breast cancer. EZH2 is significantly increased in invasive carcinoma and breast cancer metastases at both the transcript and protein levels when compared with normal breast tissues. Cells forming intravascular tumor emboli had strikingly increased EZH2 expression (Fig. 1*c Left*), suggesting that EZH2 may play a role in vascular invasion and breast cancer metastasis. *In vitro* and *in vivo* experiments in which EZH2 was ectopically overexpressed in normal mammary epithelial cell lines provide biological evidence that EZH2 can mediate anchorage-independent growth and cell membrane invasion, hallmarks of cancer (36). This is especially intriguing in that EZH2, which targets transcriptional repression of target genes, presumably mediates an invasive cancer phenotype.

To test the clinical utility of EZH2 protein expression as a prognostic biomarker of breast cancer progression, we evaluated the associations between EZH2 and survival afer treatment. At the univariate level, EZH2, tumor stage, tumor size, the presence of axillary lymph node metastases, and hormone receptor status were all significantly associated with survival. In a multivariable Cox regression analysis, high EZH2 expression and lymph node metastasis were independent predictors of outcome. The single best multivariable model included high EZH2 levels, positive lymph nodes, and negative PR status. *In silico* analysis of the cDNA expression profiling of breast cancer performed by van't Veer *et al.* (30) showed that high EZH2 levels were associated with the development of metastasis within 5 years of primary diagnosis in

patients with sporadic invasive carcinomas. These findings support the potential clinical utility of incorporating EZH2 into clinical nomograms to help determine the risk of cancer progression.

A major limitation of our analysis is its retrospective nature, which precludes an accurate analysis of survival in the context of hormonal or adjuvant treatment. In our patient cohort, 88% ER-positive tumors received hormonal treatment. Thus, we critically evaluated the prognostic significance of EZH2, taking into account tumor ER status. EZH2 was strongly associated with clinical outcome in hormone-dependent and -independent breast cancer patients, indicating that the prognostic power of EZH2 is independent of ER status. Future studies will test the model developed in this study on a validation cohort to confirm these initial observations.

The prognostic significance of EZH2 as biomarker for aggressive breast cancer is likely linked to its biological functions. EZH2 is a member of a group of polycomb proteins that are involved in maintaining heritable gene expression profiles and thus regulate cell type identity. Thus, dysregulation of the transcriptional machinery of a cell may result in loss of cell type identity and neoplastic transformation. Here we provide biological evidence that dysregulated EZH2 promotes oncogenic transformation. Overexpression of EZH2 in breast epithelial cells induced anchorage-independent growth and cell invasion. Invasive properties of EZH2 overexpressing cells were demonstrated in both *in vitro* assays (i.e., basement membrane invasion chamber and SU-ECM assays) as well as in an *in vivo* assay (i.e., CAM). EZH2 overexpression induced HDAC enzymatic activity in breast epithelial cells. Interestingly, EZH2-mediated cell invasion are abrogated by the HDAC inhibitors TSA and SAHA, implying that EZH2-mediated invasion requires HDAC activity. Previous reports have shown that type I HDACs are recruited to the EZH2-EED PcG complex (18). Our group and other groups have found that EZH2-mediated gene silencing requires an intact SET domain and recruitment of HDAC activity (8), and that inhibition of HDAC activity blocked the transcriptional repressor functions of EZH2. Several HDAC inhibitors, including SAHA, have been shown to have promise clinically as antitumorigenic agents (37). Thus, we suggest that inhibitors of HDAC may be useful therapeutic compounds in EZH2 overexpressing tumors. In addition, the HDAC activity induced by EZH2 may explain the intriguing strong association between EZH2 protein expression and negative ER, and one might speculate that EZH2 may transcriptionally repress ER. Further investigation in this area may be warranted.

Several recent studies provide strong evidence that EZH2 has inherent activity as a histone H3 methyltransferase, which may represent the mechanism of PcG silencing (10, 13–15). Cao *et al.* (13) present evidence that the specific target of EZH2 is lysine 27 on the histone H3 N-terminal tail (13). If EZH2 plays a role in breast cancer progression, its inherent methyltransferase activity may serve as an attractive therapeutic target. Together, these studies suggest that the transcriptional memory machinery of a cell may have a role in cancer progression.

In summary, we discovered that EZH2 is a promising biomarker of aggressive breast cancer, not only extending our initial observations in prostate cancer but also suggesting that EZH2 (and thus the cell memory machinery) may have a role in carcinoma progression in malignancies from hormonally regulated tissues. Clinically, our retrospective studies suggest that EZH2 levels can be used to identify patients with breast cancer of a more aggressive phenotype, thereby enhancing our prognostic knowledge. Although our results are promising, EZH2 expression needs to be validated in relationship to outcome in the context of carefully controlled clinical trials. If confirmed, application of EZH2 immunohistochemical analysis should be technically straightforward and feasible. In addition to the potential prognostic utility of EZH2, we also provide a biologic mechanism for its association with aggressive cancers, by mediating anchorage-independent growth and cell invasion.

We thank M. Wicha for helpful suggestions and S. Merajver for helpful discussions, substantive revisions of the text, and support of C.G.K.'s research. We also thank S. Ethier (University of Michigan, Ann Arbor) for breast epithelial cell lines, T. Jenuwein (Research Institute of Molecular Pathology, Vienna) for the EZH2 plasmid, K. Hamer for antibody production and purification, J. Wolf for tissue microarray construction, S. Markwart for technical assistance, S. Bhagavathula for database support, and T. Lamigan and the Vector Core for adenovirus generation. A.M.C. is a Pew Foundation Scholar, and S.A.T. is supported by the Medical Scientist Training Program. This work was supported in part by Department of Defense Grants DAMD17-02-1-0490 and DAMD17-02-1-491 (to C.G.K.); a Munn Grant from the University of Michigan (to C.G.K.); a Breast Cancer Research Foundation grant (to A.M.C.); a grant from the Mary Kay Ash Foundation (to A.M.C.); a grant from the V Foundation (to A.M.C.); National Institutes of Health Grant RO1 CA97063 (to A.M.C., D.G., and M.A.R.); and National Institutes of Health Grant P50CA69568 (to A.M.C., D.G., and M.A.R.).

1. Jemal, A., Murray, T., Samuels, A., Ghafoor, A., Ward, E. & Thun, M. J. (2003) *CA Cancer J. Clin.* **53**, 5–26.
2. Ellis, M., Hayes, D. & Lippman, M. (2000) in *Diseases of the Breast*, eds. Harris, J., Lippman, M. E. & Morrow, M. (Lippincott–Raven, Philadelpha), pp. 749–798.
3. Hayes, D. F., Isaacs, C. & Stearns, V. (2001) *J. Mammary Gland Biol. Neoplasia* **6**, 375–392.
4. Hayes, D. F., Trock, B. & Harris, A. L. (1998) *Breast Cancer Res. Treat.* **52**, 305–319.
5. Honig, S. (1996) in *Diseases of the Breast*, eds. Harris, J. L. M., Morrow, M. & Hellman, S. (Lippincott–Raven, Philadelphia), pp. 461–485.
6. Clark, G. M. (1996) in *Diseases of the Breast*, eds. Harris. J. L. M.., Morrow, M. & Hellman, S. (Lippincott–Raven, Philadephia), pp. 461–485.
7. Hayes, D. F. (2000) *Eur. J. Cancer* **36**, 302–306.
8. Varambally, S., Dhanasekaran, S. M., Zhou, M., Barrette, T. R., Kumar-Sinha, C., Sanda, M. G., Ghosh, D., Pienta, K. J., Sewalt, R. G., Otte, A. P., *et al.* (2002) *Nature* **419**, 624–629.
9. Laible, G., Wolf, A., Dorn, R., Reuter, G., Nislow, C., Lebersorger, A., Popkin, D., Pillus, L. & Jenuwein, T. (1997) *EMBO J.* **16**, 3219–3232.
10. Satijn, D. P. & Otte, A. P. (1999) *Biochim. Biophys. Acta* **1447**, 1–16.
11. Jacobs, J. J., Kieboom, K., Marino, S., DePinho, R. A. & van Lohuizen, M. (1999) *Nature* **397**, 164–168.
12. Jacobs, J. J., Scheijen, B., Voncken, J. W., Kieboom, K., Berns, A. & van Lohuizen, M. (1999) *Genes Dev.* **13**, 2678–2690.
13. Cao, R., Wang, L., Wang, H., Xia, L., Erdjument-Bromage, H., Tempst, P., Jones, R. S. & Zhang, Y. (2002) *Science* **298**, 1039–1043.
14. Czermin, B., Melfi, R., McCabe, D., Seitz, V., Imhof, A. & Pirrotta, V. (2002) *Cell* **111**, 185–196.
15. Muller, J., Hart, C. M., Francis, N. J., Vargas, M. L., Sengupta, A., Wild, B., Miller, E. L., O'Connor, M. B., Kingston, R. E. & Simon, J. A. (2002) *Cell* **111**, 197–208.
16. Shao, Z., Raible, F., Mollaaghababa, R., Guyon, J. R., Wu, C. T., Bender, W. & Kingston, R. E. (1999) *Cell* **98**, 37–46.
17. Sewalt, R. G., van der Vlag, J., Gunster, M. J., Hamer, K. M., den Blaauwen, J. L., Satijn, D. P., Hendrix, T., van Driel, R. & Otte, A. P. (1998) *Mol. Cell. Biol.* **18**, 3586–3595.
18. van der Vlag, J. & Otte, A. P. (1999) *Nat. Genet.* **23**, 474–478.
19. Tie, F., Furuyama, T., Prasad-Sinha, J., Jane, E. & Harte, P. J. (2001) *Development (Cambridge, U.K.)* **128**, 275–286.
20. Sewalt, R. G., Lachner, M., Vargas, M., Hamer, K. M., den Blaauwen, J. L., Hendrix, T., Melcher, M., Schweizer, D., Jenuwein, T. & Otte, A. P. (2002) *Mol. Cell. Biol.* **22**, 5539–5553.
21. Dhanasekaran, S. M., Barrette, T. R., Ghosh, D., Shah, R., Varambally, S., Kurachi, K., Pienta, K. J., Rubin, M. A. & Chinnaiyan, A. M. (2001) *Nature* **412**, 822–826.
22. Perrone, E. E., Theoharis, C., Mucci, N. R., Hayasaka, S., Taylor, J. M., Cooney, K. A. & Rubin, M. A. (2000) *J. Natl. Cancer Inst.* **92**, 937–939.
23. Camp, R. L., Charette, L. A. & Rimm, D. L. (2000) *Lab. Invest.* **80**, 1943–1949.
24. Zhou, M., Chinnaiyan, A. M., Kleer, C. G., Lucas, P. C. & Rubin, M. A. (2002) *Am. J. Surg. Pathol.* **26**, 926–931.
25. Livant, D. L., Linn, S., Markwart, S. & Shuster, J. (1995) *Cancer Res.* **55**, 5085–5093.
26. Morris, V. L., Koop, S., MacDonald, I. C., Schmidt, E. E., Grattan, M., Percy, D., Chambers, A. F. & Groom, A. C. (1994) *Clin. Exp. Metastasis* **12**, 357–367.
27. Rhodes, D. R., Barrette, T. R., Rubin, M. A., Ghosh, D. & Chinnaiyan, A. M. (2002) *Cancer Res.* **62**, 4427–4433.
28. Perou, C. M., Sorlie, T., Eisen, M. B., van de Rijn, M., Jeffrey, S. S., Rees, C. A., Pollack, J. R., Ross, D. T., Johnsen, H., Akslen, L. A., *et al.*. (2000) *Nature* **406**, 747–752.
29. Hedenfalk, I., Duggan, D. D., Chen, Y., Radmacher, M., Bittner, M., Simon, R., Meltzer, P., Gusterson, B. A., Esteller, M., Kallioniemi, O. P., *et al.* (2001) *New Engl. J. Med.* **344**, 539–548.
30. van't Veer, L. J., Dai, H., van de Vijver, M. J., He, Y. D., Hart, A. A., Mao, M., Peterse, H. L., van der Kooy, K., Marton, M. J., Witteveen, A. T., *et al.* (2002) *Nature* **415**, 530–536.
31. Gruvberger, S., Ringner, M., Chen, Y., Panavally, S., Saal, L. H., Borg, A., Ferno, M., Peterson, C. & Meltzer, P. S. (2001) *Cancer Res.* **61**, 5979–5984.
32. Sorlie, T., Perou, C. M., Tibshirani, R., Aas, T., Geisler, S., Johnsen, H., Hastie, T., Eisen, M. B., van de Rijn, M., Jeffrey, S. S., *et al.* (2001) *Proc. Natl. Acad. Sci. USA* **98**, 10869–10874.
33. Raaphorst, F. M., van Kemenade, F. J., Blokzijl, T., Fieret, E., Hamer, K. M., Satijn, D. P., Otte, A. P. & Meijer, C. J. (2000) *Am. J. Pathol.* **157**, 709–715.
34. Ignatoski, K. M., Lapointe, A. J., Radany, E. H. & Ethier, S. P. (1999) *Endocrinology* **140**, 3615–3622.
35. Livant, D. L., Brabec, R. K., Pienta, K. J., Allen, D. L., Kurachi, K., Markwart, S. & Upadhyaya, A. (2000) *Cancer Res.* **60**, 309–320.
36. Hanahan, D. & Weinberg, R. A. (2000) *Cell* **100**, 57–70.
37. Huang, L. & Pardee, A. B. (2000) *Mol. Med.* **6**, 849–866.